

# Modeling biochar effects on soil organic carbon on croplands in a microbial decomposition model (MIMICS-BC\_v1.0)

Mengjie Han<sup>1,2,3</sup>, Qing Zhao<sup>2,3,4</sup>, Xili Wang<sup>6</sup>, Ying-Ping Wang<sup>7</sup>, Philippe Ciais<sup>8</sup>, Haicheng Zhang<sup>9</sup>, Daniel S. Goll<sup>8</sup>, Lei Zhu<sup>1</sup>, Zhe Zhao<sup>1</sup>, Zhixuan Guo<sup>1</sup>, Chen Wang<sup>10</sup>, Wei Zhuang<sup>11</sup>, Fengchang Wu<sup>12</sup>, Wei Li<sup>1,5\*</sup>

5 <sup>1</sup>Department of Earth System Science, Ministry of Education Key Laboratory for Earth System Modeling, Institute for Global Change Studies, Tsinghua University, Beijing 100084, China.

<sup>2</sup>Guangdong Key Laboratory of Integrated Agro-environmental Pollution Control and Management, Institute of Eco-environmental and Soil Sciences, Guangdong Academy of Sciences, Guangzhou 510650, China.

10 <sup>3</sup>Key Laboratory of Pollution Ecology and Environmental Engineering Institute of Applied Ecology; Institute of Applied Ecology, Chinese Academy of Sciences, Shenyang 110016, China.

<sup>4</sup>National-Regional Joint Engineering Research Center for Soil Pollution Control and Remediation in South China, Guangzhou 510650, China.

<sup>5</sup>Institute for Carbon Neutrality, Tsinghua University, Beijing 100084, China.

<sup>6</sup>Economic & Information center, Zhejiang, China.

15 <sup>7</sup>CSIRO Environment, Private Bag 10, Clayton South VIC 3169 Australia.

<sup>8</sup>Laboratoire des Sciences du Climat et de l'Environnement, LSCE/IPSL, CEA-CNRS-UVSQ, Université Paris Saclay, 91191, Gif sur Yvette, France.

<sup>9</sup>Sun Yat Sen Univ, Sch Geog & Planning, Guangzhou, Peoples R China.

20 <sup>10</sup>Key Laboratory of Vegetation Restoration and Management of Degraded Ecosystem, South China Botanical Garden, Chinese Academy of Sciences, Guangzhou, China.

<sup>11</sup>Guangdong Institute of Engineering Technology Research Co., Ltd, Guangzhou 510440, China.

<sup>12</sup>State Key Laboratory of Environmental Criteria and Risk Assessment, Chinese Research Academy of Environmental Sciences, Beijing 100012, China.

25 \*Correspondence to: Wei Li ([wli2019@tsinghua.edu.cn](mailto:wli2019@tsinghua.edu.cn))

**Abstract.** Biochar (BC) application in croplands aims to sequester carbon and improve soil quality, but its impact on soil organic carbon (SOC) dynamics is not represented in most land models used for assessing land-based climate mitigation, therefore we are unable to quantify the effects of biochar applications under different climate conditions or land management. To fill this gap, here we implement a submodel to represent biochar into a microbial decomposition model named MIMICS (MIcrobial-MIneral Carbon Stabilization). We first calibrate and validate MIMICS with new representations of density-dependent microbial turnover rate, adsorption of available organic carbon on mineral soil particles, and soil moisture effects on decomposition using global field measured cropland SOC at 285 sites. We further integrate biochar in MIMICS by accounting for its effect on microbial decomposition and SOC sorption/desorption and optimize two biochar-related parameters in these processes using 134 paired SOC measurements with and without biochar addition. The MIMICS-biochar version can generally reproduce the short-term ( $\leq 6$  yr) and long-term (8 yr) SOC changes after adding biochar (mean addition rate:  $25.6 \text{ t ha}^{-1}$ ) ( $R^2 = 0.79$  and  $0.97$ ) with a low root mean square error (RMSE =  $3.73$  and  $6.08 \text{ g kg}^{-1}$ ). Our study incorporates sorption and soil moisture processes into MIMICS and extends its capacity to simulate biochar decomposition, providing a

useful tool to couple with dynamic land models to evaluate the effectiveness of biochar applications on removing CO<sub>2</sub> from the atmosphere.

## 40 1. Introduction

Soil organic carbon (SOC) is the largest terrestrial carbon pool, and increasing soil respiration in response to global warming can cause large carbon emissions to the atmosphere (Bond-Lamberty et al., 2018). On the other hand, SOC sequestration through improved land management practices has a potential to mitigate climate change by increasing soil carbon accumulation, such as the “4 per mille” project (Minasny et al., 2017). Due to the limited temporal and spatial coverage of field  
45 SOC measurements, soil biogeochemical models have been widely applied to simulate SOC and its response to climate change and human activities (Eglin et al., 2010). Soil carbon models are evolving from first-order kinetics-based models with simple representation of pool sizes and their turnover rates to microbial models with explicit representation of microbial roles in SOC decomposition and stabilization (Manzoni and Porporato, 2009; Sulman et al., 2018). For example, the MIcrobial-MIneral Carbon Stabilization (MIMICS) model is a process-based soil carbon model with explicit representations of nonlinear SOC  
50 decomposition dynamics related to microbial physiology, substrate quality, and physical protection of SOC (Wieder et al., 2014; Wieder et al., 2015). This model has been calibrated with global SOC data and can well represent current understanding of SOC decomposition and formation (Wieder et al., 2015), and outperforms conventional first-order decomposition model in simulating spatial variation in SOC stocks in forest ecosystems on continental scale (Zhang et al., 2020). However, the model has not been evaluated for agricultural sites or misses processes that theoretically should influence SOC dynamics.

55

The microbial interactions at the community level (e.g., competition) play a crucial role in controlling SOC dynamics, but they are usually omitted in microbial models (Georgiou et al., 2017), resulting in unrestricted growth of microbial community size with more carbon input which is unrealistic (Buchkowski et al., 2017; Wieder et al., 2013). In addition, field experiments show that physicochemical adsorption plays a more important role in controlling DOC fluxes than the biodegradation process  
60 (Kalbitz et al., 2005). Although the adsorption mechanism is complex, depending on various factors such as pH, clay content, destruction and formation of soil aggregates (Mayes et al., 2012), some soil carbon models implemented dynamic adsorption and desorption processes controlled by DOC concentration and available mineral surface sites for binding (Wang et al., 2020a; Wang et al., 2013). The availability of SOC is influenced by the adsorption process (Michalzik et al., 2003). Some adsorption kinetic equations, such as the Langmuir isotherm, have commonly been employed to depict the adsorption/desorption process.  
65 However, the MIMICS model lacks consideration of the adsorption process, thus not effectively elucidating its role in stabilizing SOC. Furthermore, the effect of soil moisture on SOC cannot be ignored because it controls microbial activity, substrate availability and further influences soil respiration and nitrogen mineralization (Manzoni et al., 2012; Schimel et al., 2007). A set of empirical functions for the soil moisture effects were proposed for the use in earth system models (ESMs)

(Moyano et al., 2013; Camino-Serrano et al., 2018), and a mechanistic moisture function that incorporates physicochemical and biological processes was also developed recently (Yan et al., 2018). In previous MIMICS versions, an implicit or explicit microbial density dependent turnover was introduced (Wieder et al. 2015; Kyker-Snowman et al. 2020; Zhang et al., 2020; Georgiou et al. 2017), which cause an increase in microbial biomass turnover with increasing microbial community size reflecting increasing pressure from competition for other resource other than carbon (e.g. space) and virus infections (Jansson and Wu, 2023), and a water scalar was used to represent the soil moisture effects (Wieder et al. 2019). The inclusion of density-dependent microbial turnover rate improved the accuracy of predicting SOC at the global scale compared to MIMICS without it and eliminated the correlation between simulated biases and input of annual litterfall (Zhang et al., 2020). MIMICS with soil water modifications showed comparable predicted global soil carbon stocks compared to other models, but to what extent soil water influences SOC turnover remains uncertain (Wieder et al., 2019). Therefore, based on these theories and model limitations, it is necessary to integrate the three aspects (density-dependent microbial turnover rate, adsorption/desorption processes, and soil moisture impacts) into one model version to improve the prediction accuracy of SOC dynamics. For agricultural lands, modeling the SOC decomposition processes is more challenging due to management practices such as tillage and fertilization, which can significantly interrupt carbon cycle and need specific parameterizations.

Biochar application in croplands as a soil amendment can improve the soil quality and increase the crop production (Smith, 2016; Woolf et al., 2010). Meanwhile, because biochar is produced from biomass through pyrolysis processes and is recalcitrant to be decomposed, it is also considered as a promising negative emission technology (NET) for climate mitigation (Fuss et al., 2018; Minx et al., 2018). The carbon dioxide removal (CDR) potential of biochar is estimated to be 0.5~2 GtCO<sub>2</sub>e year<sup>-1</sup> (CO<sub>2</sub> equivalent) (Fuss et al., 2018; Minx et al., 2018). However, biochar application affects SOC mineralization through various processes (Palansooriya et al., 2019; Luo et al., 2017), resulting in positive or negative priming effects (PEs, changes of native SOC mineralization) (Zimmerman et al., 2011). A recent meta-analysis showed that biochar induced negative priming effects on average (-3.8%), but the 95% confidence interval (CI) of -8.1% to 0.8% also covers positive values (Wang et al., 2016). Biochar may induce positive PEs through stimulating microbial activity by providing additional nutrients for soil microbes (El-Naggar et al., 2019; Li et al., 2019). Positive PEs usually occurred in shorter term (< 2 year), then decreased or changed to being negative over longer term (Luo et al., 2011; Singh and Cowie, 2014; Ding et al., 2017). For example, biochar can reduce SOC available for microbes by enhancing soil aggregate stability through associations between soil minerals and biochar (Zheng et al., 2018). Its porous structure and high surface area with strong adsorption affinity for SOC can thus cause negative PEs (Zimmerman et al., 2011; Lehmann et al., 2021). PEs are also impacted by the properties of biochar (e.g., feedstock type, pyrolysis temperature) and soil climate (e.g., soil moisture) (Ding et al., 2017). Therefore, soil moisture could be closely related to the adsorption capacity of biochar, and needs to be included in the model for predicting PEs of biochar on SOC changes. The biochar decomposition and impacts on native SOC through priming effects are important for the CDR

potential of biochar, but these processes are not represented in most land carbon models (Lehmann et al., 2021), precluding the model capacity of fully assessing the effectiveness of large-scale application of biochar as a NET and its environmental impacts.

## 2. Materials and methods

### 105 2.1 Modifications of the MIMICS model

#### 2.1.1 The default version of MIMICS (MIMICS-def)

There are seven carbon pools in MIMICS: two litter pools, two microbial biomass pools and three SOC pools (Fig. 1). The litter inputs (LIT) are divided into metabolic (LIT<sub>m</sub>) and structural pools (LIT<sub>s</sub>) according to the litter quality ( $f_{met}$ , i.e., fraction of litter to LIT<sub>m</sub>), which is linearly related to the ratio of lignin to nitrogen (lignin:N, Table S1). Microbial growth efficiency (MGE) determines the carbon fluxes from the two litter pools and the available SOC pool (SOC<sub>a</sub>) for microbial biomass pools and heterotrophic respiration. The turnover of microbial biomass ( $\tau$ ) depends on the functional types of soil microbes (MIC<sub>r</sub> and MIC<sub>k</sub> for r- and k-strategy, respectively). Three SOC pools represent the available (SOC<sub>a</sub>), physically protected (SOC<sub>p</sub>) and chemically recalcitrant SOC (SOC<sub>c</sub>). SOC in the protected pools (i.e., SOC<sub>p</sub> and SOC<sub>c</sub>) are released to the available SOC pool (SOC<sub>a</sub>) over time. More detailed description of the model parameters and carbon fluxes can be found in Table S1 and  
 110 Wieder et al. (2015). The carbon decomposition rate ( $\text{mg C cm}^{-3} \text{ hr}^{-1}$ ) of the litter and SOC pools is based on a temperature-sensitive Michaelis–Menten kinetics (Allison et al., 2010; Schimel and Weintraub, 2003):

$$\frac{dC_s}{dt} = MIC \times \frac{V_{max} \times C_s}{K_m + C_s} \quad (1)$$

where  $C_s$  ( $\text{mg C cm}^{-3}$ ) is the size of a substrate carbon pool (LIT or SOC), and  $MIC$  ( $\text{mg C cm}^{-3}$ ) is the size of the microbial carbon pool (MIC<sub>r</sub> or MIC<sub>k</sub>).  $V_{max}$  and  $K_m$  are the microbial maximum reaction velocity ( $\text{mg C (mg MIC)}^{-1} \text{ hr}^{-1}$ ) and the  
 120 half-saturation constant ( $\text{mg C cm}^{-3}$ ), respectively, which depend on temperature,  $T$ , in °C.

$$V_{max} = e^{V_{slope}T + V_{int}} \times a_v \times V_{mod} \quad (2)$$

$$K_m = e^{K_{slope}T + K_{int}} \times a_k \times K_{mod} \quad (3)$$

where  $V_{mod}$  and  $K_{mod}$  represent the modifications of  $V_{max}$  and  $K_m$  based on their dependence on litter quality, microbial functional types, and soil texture.  $a_v$  and  $a_k$  are the tuning coefficients of  $V_{max}$  and  $K_m$ , respectively.  $V_{slope}$  and  $K_{slope}$  are the  
 125 regression coefficients, and  $V_{int}$  and  $K_{int}$  are the regression intercepts.

The turnover of MIC<sub>r</sub> and MIC<sub>k</sub> (MIC <sub>$\tau$</sub> ,  $\text{mg C cm}^{-3} \text{ hr}^{-1}$ ) at each time step depends on their specific turnover rate ( $k_{mic}$ ,  $\text{hr}^{-1}$ ), annual total litter input (LIT<sub>tot</sub>,  $\text{g C m}^{-2} \text{ year}^{-1}$ ) and  $f_{met}$ :

$$MIC_{\tau} = a_{\tau} \times k_{mic} \times e^{c f_{met}} \times \max(\min(\sqrt{LIT_{tot}}, 1.2), 0.8) \times MIC \quad (4)$$

130 where  $a_{\tau}$  (=1.0, dimensionless) is the tuning coefficient of  $k_{mic}$ .  $c$  is the regression coefficient of  $MIC_{\tau}$  (0.3) and  $MIC_k$  (0.1). The carbon inputs from microbial biomass to SOC pools are determined by the microbial biomass turnover.

The carbon transfer from  $SOC_p$  to  $SOC_a$  ( $D$ ,  $mg\ C\ cm^{-3}\ hr^{-1}$ ) represents the desorption of  $SOC_p$  from mineral surfaces or the breakdown of aggregates, calculated as a function of soil clay content ( $f_{clay}$ ):

$$135\ D = 1.5 \times 10^{-5} \times k_d \times e^{-1.5 f_{clay}} \quad (5)$$

where  $k_d$  (=1.0, dimensionless) is a tuning coefficient of the desorption rate. The parameter values of the default MIMICS version can be found in Table S1.

### 2.1.2 MIMICS considering density-dependent microbial turnover rate (MIMICS-T)

Similar to the logistic growth model in population ecology, various regulatory mechanisms (e.g., competition, virus) can limit  
 140 microbial population size (Buchkowski et al., 2017, Jansson and Wu, 2023). The absence of restrictions on population size other than carbon results in predictions of microbial biomass increasing indefinitely with carbon inputs. Consequently, the response of predicted SOC to changes in carbon inputs is close to zero which contradicts field observations (Georgiou et al., 2017). A density-dependent microbial turnover rate with  $\beta > 1$  was adopted to regulate the responses of soil microbial biomass to external environment variations, such as carbon input, thereby SOC dynamics in previous microbial models (Georgiou et al.,  
 145 2017, Zhang et al., 2020). We incorporated the density-dependent microbial turnover rate into MIMICS following Zhang et al. (2020). In the MIMICS-T version, we modified Eq. 4 to represent the increased microbial turnover rate with growing microbial biomass density ( $MIC$ ,  $mg\ C\ cm^{-3}$ ):

$$MIC_{\tau} = a_{\tau} \times k_{mic} \times e^{c \times f_{met}} \times \max(\min(\sqrt{LIT_{tot}}, 1.2), 0.8) \times MIC^{\beta} \quad (6)$$

where  $\beta$  is the density-dependence exponent.

### 150 2.1.3 MIMICS-T with additional representation of sorption (MIMICS-TS)

Although the MIMICS model can simulate the desorption process (the yellow arrow from  $SOC_p$  to  $SOC_a$ , Fig. 1), the adsorption process is still missing. In the original version of MIMICS, fixed fractions of litter and microbial turnover are transferred to the physically protected SOC pool ( $SOC_p$ , Fig. 1), the  $SOC_p$  is then deprotected from mineral surfaces or breakdown of aggregates using a desorption rate which is a function of clay fraction. Therefore, we do not think that the  
 155 original MIMICS actually simulates sorption as a process, as sorption is dependent on substrate concentration, therefore the sorption rate should vary with dissolved organic carbon concentration, rather than being proportional to microbial carbon

turnover rate as assumed in the original MIMICS. Therefore, we further added the adsorption of available SOC into MIMICS following Wang et al. (2013) and Mayes et al. (2012). The MIMICS-TS version includes a new sorption process (the purple arrow from SOC<sub>a</sub> to SOC<sub>p</sub> in Fig. 1) but keeps the original desorption process (i.e., the yellow arrow from SOC<sub>p</sub> to SOC<sub>a</sub> in Fig. 1) unchanged. The sorption capacity of SOC<sub>a</sub> (Q<sub>max</sub>) increases with increasing clay content, and the carbon flux of the sorption process is calculated as follows:

$$F_{ads} = K_{ads} \times \left(1 - \frac{SOC_p}{Q_{max}}\right) \times SOC_a \quad (7)$$

$$K_{ads} = k_d \times k_{ba} \quad (8)$$

$$Q_{max} = 10^{(c_1 \times \log(\%clay) + c_2)} \quad (9)$$

where  $F_{ads}$  is the carbon flux from SOC<sub>a</sub> to SOC<sub>p</sub> (mg C cm<sup>-3</sup> hr<sup>-1</sup>).  $k_{ba}$  is the binding affinity, and  $K_{ads}$  is the sorption rate of SOC<sub>p</sub> which is associated with the desorption rate ( $k_d$ ).  $Q_{max}$  is the maximum sorption capacity of SOC<sub>p</sub> (mg C cm<sup>-3</sup> soil).  $c_1$  and  $c_2$  are the coefficient for estimating  $Q_{max}$  from Mayes et al. (2012).

#### 2.1.4 MIMICS-TS with soil moisture effects (MIMICS-TSM)

Finally, based on MIMICS-TS, we added soil moisture effects on decomposition into MIMICS. We tested two empirical functions for soil moisture used respectively in the Century model (Parton et al., 2000, Eq. 10) and the ORCHIDEE-SOM model (Camino-Serrano et al., 2018, Eq. 11). We also attempted to implement one mechanism-based function that captures the main physicochemical and biological processes of soil moisture in regulating soil respiration from Yan et al. (2018) (Eq. 12). The three functions of soil moisture are illustrated in Fig. S1.

$$f_{m1}(w) = \frac{1}{1 + p_1 \times e^{(p_2 \times w)}} \quad (10)$$

$$f_{m2}(\theta) = \max(0.25, \min(1, k_1 \times \theta^2 + k_2 \times \theta + k_3)) \quad (11)$$

$$f_{m3}\left(\frac{\theta}{\phi}\right) = \begin{cases} \frac{K_{\theta} + \theta_{op}}{K_{\theta} + \theta} \times \left(\frac{\theta}{\theta_{op}}\right)^{(1 + a n_s)}, & \theta < \theta_{op} \\ \left(\frac{\phi - \theta}{\phi - \theta_{op}}\right)^b, & \theta \geq \theta_{op} \end{cases} \quad (12)$$

where  $f_{mi}$  ( $i=1, 2, 3$ , unitless value in range from 0 to 1) is the response factor to soil moisture.  $w$  is the soil moisture indicator (AI, mm mm<sup>-1</sup>).  $p_1$  and  $p_2$  are empirical parameters of soil moisture scalar with  $p_1 = 30$  and  $p_2 = -8.5$  (Parton et al., 2000).  $\theta$  is soil moisture (m<sup>3</sup> m<sup>-3</sup>).  $k_1$ ,  $k_2$  and  $k_3$  are soil moist coefficients with 1.1, 2.4 and 0.29, respectively (Camino-Serrano et al., 2018).  $\phi$  is the soil porosity related to soil bulk density, and  $\theta/\phi$  is the relative water content in soil pores.  $\theta_{op}$  is an optimum soil moisture content parameter at which the heterotrophic respiration rate peaks.  $K_{\theta}$  is moisture constant depending on organic-mineral associations.  $n_s$  is saturation exponent depending on soil structure and texture.  $a$  and  $b$  are SOC-microbial collocation factor and oxygen supply restriction factor, respectively (Yan et al., 2018).

185 We assumed that the kinetic parameters  $V_{max}$  and  $K_m$  respond to soil moisture, similarly to temperature in Michaelis-Menten equation by affecting enzyme activity and enzyme-substrate affinity, respectively. The soil enzyme-substrate affinity was found to increase with soil moisture due to the increased diffusion and movement of substrate, but the affinity may also decrease due to decreased substrate concentrations (Zhang et al., 2009). Thus, we translated the impacts of soil moisture on the enzyme-substrate affinity to changes in  $K_m$ . In MIMICS-TSM, the effects of soil moisture on SOC decomposition rate are  
 190 represented through multiplying the response factor by  $V_{max}$  and  $K_m$  as follows (Eq. 13, 14).

$$V_{max} = e^{V_{slope} \cdot T + V_{int}} \cdot a_v \cdot V_{mod} \times f_{mi} \quad (13)$$

$$K_m = e^{K_{slope} \cdot T + K_{int}} \cdot a_k \cdot K_{mod} \times f_{mi} \quad (14)$$

The MIMICS models with three soil moisture functions of  $f_{m1}$  (Eq. 10),  $f_{m2}$  (Eq. 11) and  $f_{m3}$  (Eq. 12) are indicated as MIMICS-TSM<sub>a</sub>, MIMICS-TSM<sub>b</sub> and MIMICS-TSM<sub>c</sub>, respectively. The modifications of all MIMICS versions are  
 195 summarized in Table 1.

### 2.1.5 Adjusted parameters for cropland SOC

Crop NPP at each site was used as the litter input to soil, but different crop types (e.g., maize, rice and wheat) were not specified in the model. The leaf, root and stem litter were assumed as a fixed fraction of crop NPP. The ratio of carbon to nitrogen (C: N) and the ratio of lignin to carbon (lignin: C) of leaf, root, and stem (Table S2) were used to calculate the  
 200 metabolic fraction in the total crop litter ( $f_{met}$ ). It was calculated as the mean metabolic fractions in leaf, root and stem, weighted by NPP in the three parts. In order to adapt MIMICS for simulating cropland SOC, we modified C:N and lignin:C in the three parts based on field measurements of main crop types (Abiven et al., 2005, Table S2). A harvest index (HI) of 0.45 (Hicke and Lobell, 2004) was also applied to remove the harvested part of crop and obtain the litter input to soil (= crop aboveground NPP  $\times$  (1-HI)).

## 205 2.2 Implementing biochar modeling in MIMICS

When applying biochar in croplands, a fraction of biochar ( $f_{loss} = 2\%$ , Archontoulis et al., 2016) was assumed to be lost during application. Although biochar is recalcitrant to decompose with a long turnover time ( $556 \pm 484$  yr) in general, it contains some labile fraction ( $108 \pm 196$  day), and its stability varies with different biochar feedstocks, pyrolysis temperatures and soil properties (Wang et al., 2016). Because the sizes of SOC<sub>p</sub> and SOC<sub>c</sub> pools in MIMICS are not measured directly in the  
 210 field studies, the 98 % remaining fraction of added biochar is partitioned into three MIMICS SOC pools by assuming that 60% goes to SOC<sub>p</sub> based on the measured proportions of added biochar within aggregates (Yoo et al., 2017), 20% goes to SOC<sub>a</sub> according to the labile C portion in biochar (Roberts et al., 2010) and 20% goes to SOC<sub>c</sub>, respectively (Fig. 1). Note that

biochar is not treated as a separate carbon pool but is assumed to mix with other carbon in the existing pools (Fig. 1). In addition to the increase of total SOC, some important processes controlling SOC accumulation and decomposition are affected by biochar addition. We thus modified the parameters related to decomposition and desorption of SOC (Fig. 1). The associated rationales, equations and parameters are described in the following sections.

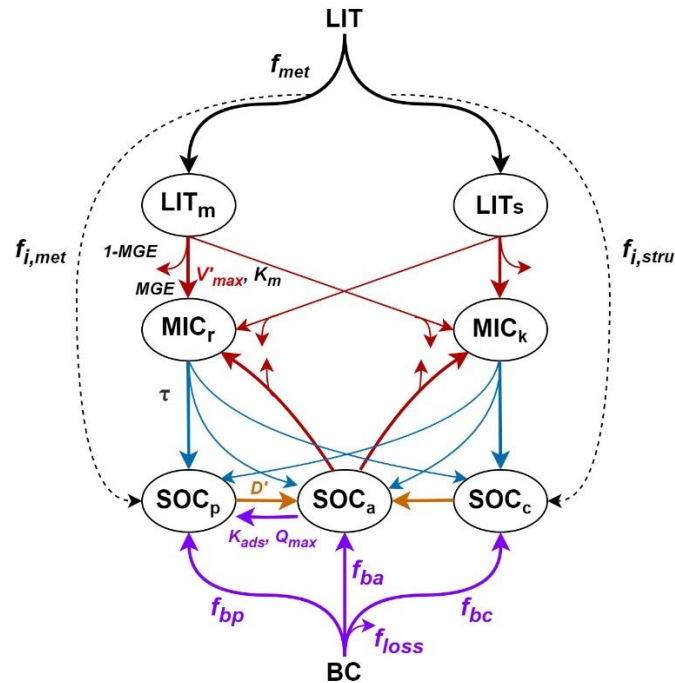


**Fig. 1** Framework of the MIMICS model with biochar addition (MIMICS-BC; adapted from Wieder et al. (2015)). The turnover of microbial biomass ( $\tau$ , blue arrows) is modified with density-dependent microbial turnover rate (Eq. 6, MIMICS-T). The adsorption process of  $\text{SOC}_p$  to  $\text{SOC}_a$  (purple arrow) is newly added and is associated with the adsorption rate ( $K_{ads}$ ) and the maximum sorption capacity ( $Q_{max}$ ) (Eq. 7-9, MIMICS-TS). The carbon decomposition processes (red arrows) are modified further with three soil moisture scalars that are applied to microbial maximum reaction velocity ( $V_{max}$ ) and the half-saturation constant ( $K_m$ ) (Eq. 10-12, MIMICS-TSM<sub>a</sub>, MIMICS-TSM<sub>b</sub>, MIMICS-TSM<sub>c</sub>). When biochar is added to soil, the biochar (BC) carbon with an assumed fraction loss ( $f_{loss}$ ) is partitioned into  $\text{SOC}_p$ ,  $\text{SOC}_a$  and  $\text{SOC}_c$  based on  $f_{bp}$ ,  $f_{ba}$  and  $f_{bc}$ , respectively (purple arrows from BC to SOC pools). The desorption process (orange arrow from  $\text{SOC}_p$  to  $\text{SOC}_a$ ) is modified through changes in the desorption rate of  $\text{SOC}_p$  ( $D'$ ) with biochar addition. The carbon decomposition processes (red arrows) are modified by adjusting the microbial maximum reaction velocity ( $V'_{max}$ ) with biochar addition.

The negative priming effects of biochar addition on SOC may be caused by the inhibition of microbial activity due to changes in the soil environments by biochar, or by the SOC protection against microbial utilization through mineral adsorption or aggregates (Zimmerman et al., 2011). We assumed that biochar addition decreased the mineralization of native SOC (negative PE) because of its porous structure and strong adsorption affinity to organic matter (Kasozi et al., 2010),



which was reported to have significantly contributed to the negative PE mechanism from biochar addition (Zheng et al., 2018; Zimmerman et al., 2011). A desorption coefficient ( $f_d$ ,  $\text{ha t}^{-1} \text{Rate\_BC}$ ) was defined as a function of the biochar application rate ( $\text{Rate\_BC}$ ) based on Woolf & Lehmann (2012) and Archontoulis et al. (2016), and Eq. 5 was thus modified as:

$$D' = D \times (1 + f_d \times \text{Rate\_BC} \times \text{BC\_C}) \quad (15)$$

where  $D'$  ( $\text{mg C cm}^{-3} \text{hr}^{-1}$ ) is the new desorption rate of  $\text{SOC}_p$  with biochar addition, and a negative value of  $f_d$  indicates a negative priming effect. The  $\text{Rate\_BC}$  is the application rate of biochar ( $\text{t BC ha}^{-1}$ ) and  $\text{BC\_C}$  is the carbon content in biochar ( $\text{t C t}^{-1}\text{BC}$ ). Because the adsorption and desorption of SOC are interrelated dynamic process, modification of the desorption process with biochar addition also impacts the adsorption process. Therefore, we only modified  $f_d$  in Eq. (15) to represent the negative PE of biochar.

We also assumed that biochar stimulated microbial growth and activity through its nutrient input, inducing a positive PE to SOC (El-Naggar et al., 2019). We defined a new decomposition rate coefficient ( $f_v$ ,  $\text{ha t}^{-1} \text{Rate\_BC}$ ) that is a function of  $\text{Rate\_BC}$ , and included it in MIMICS by modifying Eq. 2:

$$V'_{max} = V_{max} \times (1 + f_v \times \text{Rate\_BC} \times \text{BC\_C}) \quad (16)$$

where  $V'_{max}$  is the new microbial maximum reaction velocity ( $\text{mg C (mg MIC)}^{-1} \text{hr}^{-1}$ ) with biochar addition.

Biochar may also have a positive priming effect on SOC by increasing the degradation rate of available SOC by microbes (i.e.,  $\text{SOC}_a$  in MIMICS). Therefore, we added a test through modifying the  $V_{max}$  as a function of biochar addition rate only in the fluxes from  $\text{SOC}_a$  to  $\text{MIC}_r$  and  $\text{MIC}_k$ , instead of in all fluxes of decomposition (Eq. 16, red arrows in Fig. 1).

## 2.3 Model calibration and evaluation

### 2.3.1 Observational data collection

We collected 387 paired field measurements of SOC concentrations ( $\text{g kg}^{-1}$ ) in croplands with or without biochar (BC) addition from 58 locations (see the site map in Fig. 2) from published literatures. Soil properties (clay content (Clay), bulk density (BD), soil moisture (SM)), climatic conditions (mean annual temperature (MAT), mean annual precipitation (MAP)), biological variable (net primary productivity (NPP)) and biochar-related characteristics: application rate ( $\text{Rate\_BC}$ ), the interval between biochar application and soil sampling ( $\text{Age\_BC}$ ), feedstock type ( $\text{Feedstock\_BC}$ ), pyrolysis temperature ( $\text{Temp\_BC}$ ) were also collected when available. Auxiliary information (e.g., location, and managements, crop types) and more detailed information can be found in Han et al. (2021).

Because some sites have multiple biochar addition experiments (e.g., pyrolysis temperature  $\times$  aging time of biochar), the control SOC concentrations at the same site were averaged, and the SOC concentrations with biochar addition for a given rate (Rate\_BC) were also averaged, omitting other characteristics of the biochar (like pyrolysis temperature). In total, 134 paired SOC data were used for model calibration and validation (Fig. 2). The depth of soil sampled varies among sites, but is less than 30 cm in general. The biochar application rate varies from 0.9 to 120 t ha<sup>-1</sup> with a median value of 20 t ha<sup>-1</sup> (Fig. S2a). Most biochar addition experiments are short-term with the median Age\_BC of 1.2 year (Fig. S2b). The main types of cultivated crop are maize, rice and wheat.

270

There are SOC measurements on cropland sites from 58 control treatments (no BC application) and 134 measurements from biochar treatments at the 58 sites. One control treatment may correspond to multiple biochar treatments with different applied biochar rates at a single site. Considering the 58 site observations may be inadequate to constrain all the new features in the revised model, we also collected SOC data on croplands (no biochar addition) from other three published global datasets (227 sites in total, Sun et al., 2020; Geisseler et al., 2017; Zhou et al., 2017b). Therefore, 285 sites in total were used to calibrate and evaluate the model performance for simulating cropland SOC without biochar addition (Fig. 2).

Soil properties that are not reported in the literature were extracted from gridded datasets using the coordinates of the sites: clay content from Global Soil Dataset for use in Earth System Models (GSDE, Shangguan et al., 2014) and SM from the satellite observations of Soil Moisture Active Passive (SMAP, Entekhabi et al., 2010). Missing soil BD in control treatments were filled according to the relationship between SOC and bulk density based on 4765 cultivated soil data from the 2nd national soil survey (Song et al., 2005), and a decrease of 7.6% (Omondi et al., 2016) from the control soil BD was assumed to fill the missing BD values in the biochar addition experiments. The climate variable MAT was extracted from WorldClim (Fick and Hijmans, 2017), and the mean annual aridity index (AI, i.e., precipitation/potential evapotranspiration) used in the soil moisture equation (Eq. 10) was obtained from the Global Aridity Index and Potential Evapotranspiration Database (Zomer et al., 2022). The biological variable (i.e., NPP) was from the MODIS NPP dataset (Zhao and Running, 2010).

285

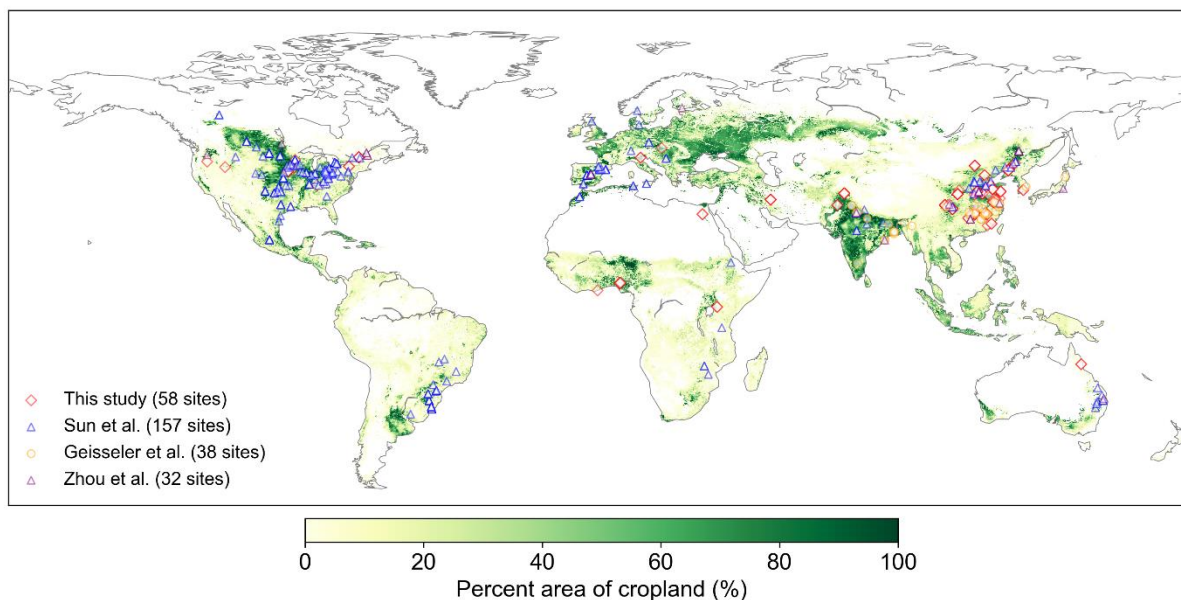


**Fig. 2** Locations of field cropland SOC measurements with or without biochar addition collected in this study and SOC measurements without biochar addition from Sun et al, (2020), Geisseler et al., (2017) and Zhou et al., (2017b). Number of sites is also shown in the legend. Note that one site may have multiple paired SOC data due to various experimental conditions of biochar addition at our collected 58 sites. The cropland area percentage in each 10 km × 10 km grid cell is derived from EarthStat (<http://www.earthstat.org>; Ramankutty et al., 2008).

### 2.3.2 Calibration and validation for MIMICS versions without biochar

All field SOC observations in the control treatments (without biochar) from the paired measurements and SOC from the other three global datasets (Fig. 2) were assumed at a steady state, which is under present climate and continuous input of crop NPP after 45% removal of grain with a specific crop litter quality (Section 2.1.5, Table S2). SOC pools in MIMICS reached an equilibrium state after about 200 years of model run (Fig. S3). To accelerate this process, we used New-Ralphson method (Press et al., 2007) to obtain the steady SOC state with the site-level inputs of annual mean crop NPP, MAT, Clay, SM and BD in the parameter optimization. This approach is constructed based on the fundamental principles governing biogeochemical cycle processes in terrestrial ecosystems (e.g., respiration, carbon distribution). A set of ordinary differential equations were built to express the dynamics of carbon flows in soil over time and it can be solved numerically to obtain steady carbon pool sizes. The solver of “*mnewt*” is used to solve equations by iteratively calculating the values of model function “*modelx*” and its Jacobian matrix “*modeljacx*” (see codes for details in **Code availability**). The Shuffled Complex Evolution Algorithm (SCE-UA) has been proven to be a robust method for parameter optimization (Duan et al., 1994; Muttil and Jayawardena, 2008), and the SCE-UA method from the *spotpy* package in python (Houska et al., 2015; <https://pypi.org/project/spotpy/>) was applied here. Parameters are optimal when the root mean square error (RMSE, Eq. 17) between simulated SOC and observed SOC concentrations is minimized. The Akaike information criterion (AIC, Eq. 18,

Akaike, 1974), which considers both model error and the number the model parameters, was also calculated to evaluate different MIMICS versions.

$$310 \quad RMSE = \sqrt{\frac{\sum_{i=1}^n (SOC_{obs,i} - SOC_{sim,i})^2}{n}} \quad (17)$$

$$AIC = n \times \ln \left( \frac{\sum_{i=1}^n (SOC_{obs,i} - SOC_{sim,i})^2}{n} \right) + 2p \quad (18)$$

Where  $SOC_{obs,i}$  and  $SOC_{sim,i}$  are the observed and simulated SOC at each  $i$  site.  $n$  is the number of observations, and  $p$  is the number of model parameters to be optimized.

315 We randomly separated 80% of all the 285 sites for the MIMICS versions (MIMICS-def, MIMICS-T, MIMICS-TS and MIMICS-TSM) calibration, and 20% for model validation. The  $R^2$ , RMSE and AIC were calculated by comparing simulated SOC with the observed SOC in training and test datasets. The parameters optimized in different MIMICS versions are shown in Table S3. Soil depth was not explicitly considered in this study, and we assumed that the soil carbon concentrations ( $g \text{ kg}^{-1}$ ) are similar within the top 30 cm. Note that the parameters of soil moisture functions (Eq. 10-12) are directly derived from the  
 320 original literature (Parton et al., 2000; Camino-Serrano et al., 2018; Yan et al., 2018) and not optimized in MIMICS-TSM. We calibrated the models against our datasets including SOC and auxiliary information (Fig. 2) for the main crop types (maize, rice, and wheat), and the relationships between SOC in these crop types and model input variables (i.e., NPP, MAT, Clay) were analyzed.

325 To explore possible soil moisture effects on SOC, we also tried a test by assuming that soil moisture affects the microbial growth rate through regulating microbial growth ( $V_{max}$ ) and turnover ( $\tau$ ) of  $MIC_r$  and  $MIC_k$  (Wieder et al., 2019) and thus added a soil moisture factor (i.e.,  $f(\theta)$  in Eq. 11) on  $V_{max}$  and  $\tau$ . The MIMICS model can run for each site, but to be consistent with the model input resolution of daily temperature in the transient simulation, the resolution of  $0.5^\circ$  was used for site aggregation. In detail, all sites within a given grid cell of  $0.5^\circ \times 0.5^\circ$  were aggregated on average, and the averaged value was  
 330 used to compare the model result in this grid cell. We also conducted a sensitivity test of MIMICS input variables (i.e., MAT, Clay, NPP, SM and BD) with four perturbation levels of -50%, -25%, 25% and 50% to explore the effects of possible underrepresented processes on the cropland steady SOC.

### 2.3.3 Calibration and validation for MIMICS versions with biochar (MIMICS-BC)

For the version of MIMICS with biochar addition, we run for each site simulations with control (without biochar addition) and  
 335 experimental simulation (with biochar addition) for Age\_BC year at hourly time steps, restarted from the previous SOC equilibrium. Note that these simulations for biochar addition are transient runs and thus SOC is not at a steady state. In order to

meet the daily time step of transient runs required by MIMICS, the two model runs are forced by 6-hour surface temperature from Climatic Research Unit and Japanese reanalysis data (CRU-JRA, Kobayashi et al., 2015; Harris et al., 2014). The climate forcing data is thus different from the one from WorldClim used for the steady runs (**Section 2.3.2**) because hourly climate data is not available in WorldClim. The soil-related inputs of Clay, SM and BD were assumed invariant in time and consistent with input data for the steady SOC runs. The absolute SOC changes ( $\Delta\text{SOC}$ ,  $\text{g kg}^{-1}$ , Eq. 19) in the simulated and observed SOC concentrations were compared after BC addition. The RMSE between simulated and observed  $\Delta\text{SOC}$  was minimized using SCE-UA for parameter optimization. AIC and the slopes of regression lines between the simulated and observed SOC changes were analyzed.

$$\Delta\text{SOC} = X_t - X_c \quad (19)$$

where  $X_t$  and  $X_c$  is the observed (or simulated) SOC concentrations with and without biochar addition, respectively.

The 134 paired observations were randomly split into training samples for parameter optimization (80% data) and test samples for model validation (20% data). One control simulation without any biochar process and three experimental simulations with different biochar processes (**Section 2.2**) were set to test the possible mechanisms of biochar impacting SOC dynamics. Four tests were conducted to evaluate the performance of MIMICS<sub>TSMb-BC</sub> on simulating SOC changes after biochar addition using the optimized parameters values in MIMICS-TSM<sub>b</sub> (i.e.,  $a_v$ ,  $a_k$ ,  $k_d$ ,  $\beta$ ,  $k_{ba}$ ,  $c_1$ ,  $c_2$ ; Table S3): 1) without biochar-related parameters (MIMICS<sub>TSMb-BC<sub>def</sub></sub>); 2) with only one new biochar-related parameter (i.e., the desorption coefficient,  $f_d$ , Eq. 15) optimized (MIMICS<sub>TSMb-BC<sub>D</sub></sub>); 3) with two new biochar-related parameters (i.e.,  $f_d$  and the decomposition rate coefficient,  $f_v$ , Eq. 16) optimized and  $f_v$  included in all decomposition processes (MIMICS<sub>TSMb-BC<sub>DV</sub></sub>); 4) with two new biochar-related parameters (i.e.,  $f_d$  and  $f_v$ ) optimized and  $f_v$  only included in the fluxes from SOC<sub>a</sub> to MIC pools (MIMICS<sub>TSMb-BC<sub>DV-SOC<sub>a</sub></sub></sub>). Although MIMICS-TSM<sub>b</sub> is not the model with the highest  $R^2$  and lowest RMSE and AIC, the differences of  $R^2$ , RMSE and AIC among various versions are relatively small (Fig. S5). The new processes (density dependent processes, sorption, and soil moisture scalars) are based on theoretical understanding and have shown to improve predictions of soil carbon in previous studies (Zhang et al., 2020, Liang et al., 2019, Abramoff et al. 2022). Thus, this version was used for further development of biochar processes in MIMICS. As an alternative model version, we also tested implementation of biochar processes in MIMICS-T that have a highest  $R^2$  and lowest RMSE and AIC in model validation (Fig. S5b). The model versions and simulation settings are shown in Table 1 and Fig. 3, and the optimized parameters values in these tests are shown in Table S3.

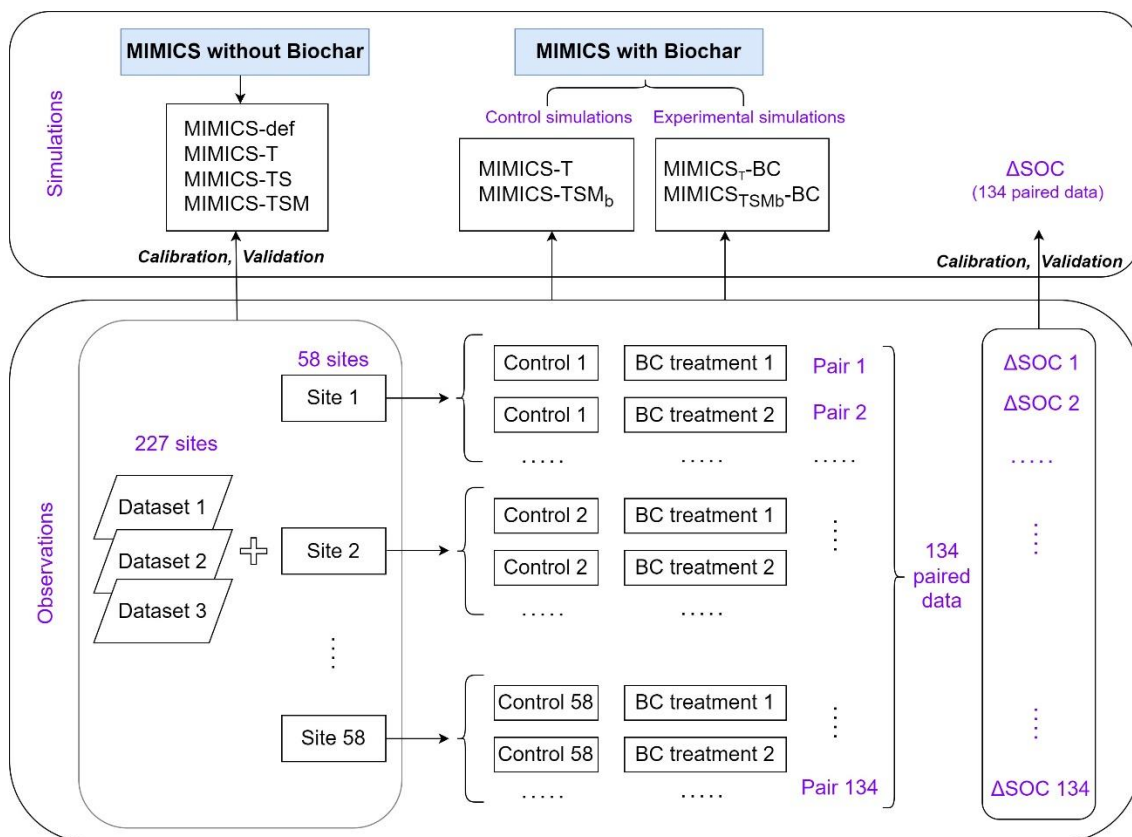
Because the duration of most biochar addition experiments is short (74.2% data < 3 years), we also extracted data with Age<sub>BC</sub>  $\geq$  3yr (4 yr, 5 yr and 6 yr) and tested the model performance on them separately. Due to lack of field measured data for a longer period, we extended our collected control SOC data to 8 years according to the decomposition curve of biochar

in soil fitted by a double first-order exponential decay model (Fig. S4; Wang et al., 2016). Note that the double exponential decay function is only applied to the observational records of measurement data, and this function is not used in the MIMICS model. Specifically, the 8-yr SOC data with biochar addition is the sum of field control SOC observations (short-term) and the residual biochar carbon in soil after 8 years. These extended long-term data were also used for model calibration and model evaluation.

The relationships between observed  $\Delta$ SOC and model input variables and the partial correlations between biases (simulated minus observed  $\Delta$ SOC) from the four tests and model input variables (soil-, climate-, biological-, and biochar-related variables) were also analyzed to detect the possible missing processes. The availability carbon in biochar may affect the magnitude of priming effects. We thus tested the MIMICS<sub>TSMb</sub>-BC versions with the partitioning coefficient from biochar carbon to SOC<sub>a</sub> ( $f_{ba}$ ) equal to 2% (Lychuk et al., 2014), and the partitioning coefficient of  $f_{bp}$  and  $f_{ba}$  were optimized to evaluate the model performance. Considering the uncertainties in the MIMICS-BC parameters, we conducted a sensitivity test of biochar-related parameters (i.e.,  $f_d$ ,  $f_v$ ,  $f_{bp}$ ,  $f_{ba}$ ), microbial-related parameters (MGE,  $\tau$ ) and input variables (i.e., Rate\_BC, Age\_BC, NPP, Clay, SM) with four perturbation levels of -50%, -25%, 25% and 50% for each site.

**Table 1** Modifications in various MIMICS versions.

Model	Model version	Description
MIMICS	MIMICS-def	The default model version with modified parameters related to crop properties ( <b>Section 2.1.5</b> ).
	MIMICS-T	Considering the density-dependent microbial turnover rate (denoted as “T”, Eq. 6).
	MIMICS-TS	Adding the sorption process of SOC <sub>p</sub> based on MIMICS-T (“S”, Eq. 7-9).
	MIMICS-TSM <sub>a</sub>	Including soil moisture effects from CENTURY model (“M <sub>a</sub> ”) based on MIMICS-TS.
	MIMICS-TSM <sub>b</sub>	Including soil moisture effects from ORCHIDEE-SOM model (“M <sub>b</sub> ”) based on MIMICS-TS.
	MIMICS-TSM <sub>c</sub>	Including soil moisture effects from Yan et al. (2018) (“M <sub>c</sub> ”) based on MIMICS-TS.
MIMICS <sub>T</sub> -BC	MIMICS <sub>T</sub> -BC <sub>def</sub>	Including the density-dependent microbial turnover rate but without biochar-related parameters for biochar addition.
	MIMICS <sub>T</sub> -BC <sub>D</sub>	Including biochar effects on SOC by modifying desorption rate of SOC <sub>p</sub> in MIMICS-T (Eq. 15).
	MIMICS <sub>T</sub> -BC <sub>DV</sub>	Including further biochar effects on SOC by modifying the microbial maximum reaction velocity in all decomposition processes in MIMICS-T (Eq. 16).
	MIMICS <sub>T</sub> -BC <sub>DV-SOC<sub>a</sub></sub>	Including further biochar effects on SOC by modifying the microbial maximum reaction velocity only in microbial decomposition of SOC <sub>a</sub> in MIMICS-T (Eq. 16).
MIMICS <sub>TSMb</sub> -BC	MIMICS <sub>TSMb</sub> -BC <sub>def</sub>	Including the density-dependent microbial turnover rate, sorption process and soil moisture effects but without biochar related parameters for biochar addition.
	MIMICS <sub>TSMb</sub> -BC <sub>D</sub>	Similar to MIMICS <sub>T</sub> -BC <sub>D</sub> but biochar is added in MIMICS-TSM <sub>b</sub> .



385

**Fig. 3** Diagram of field measurement SOC data and the model simulation settings. The simulated or observed  $\Delta$ SOC is equal to SOC with the biochar addition treatment minus that in the control treatment (without biochar addition). Note that one control treatment may correspond to multiple BC treatments with different applied BC rates at one single site.

### 3. Results of model calibration and validation

#### 390 3.1 Performance of different MIMICS versions for simulating cropland SOC

##### 3.1.1 Calibration and validation for MIMICS versions without biochar

Among the MIMICS versions without biochar related processes, MIMICS-T has the highest correlation ( $R^2=0.45$ ), the lowest RMSE (RMSE=5.81 g kg<sup>-1</sup>) and lowest AIC (AIC=810.0) between the observed and simulated cropland SOC concentrations in the model calibration (Fig. 4, Fig. S5a). Compared to MIMICS-def ( $R^2=0.43$ , RMSE=5.89 g kg<sup>-1</sup>, AIC=814.8, Fig. S5a),  
 395 other MIMICS versions show better performances in calibration with a higher  $R^2$  and lower RMSE except for MIMICS-TSM<sub>a</sub> (Fig. S5a). After considering the density-dependent microbial turnover rate, MIMICS-T can better capture the observed spatial variation of SOC (Fig. 4, Fig. S5a). MIMICS-TS with alternative implementation of SOC<sub>p</sub> adsorption explains 44% SOC

spatial variation with a smaller RMSE ( $5.81 \text{ g kg}^{-1}$ ), but a larger AIC (816.6) (Fig. 4, Fig. S5a). Compared with MIMICS-TS, the MIMICS-TSM versions that account for the effects of soil moisture do not show significantly improvement (Fig. 4; Fig. 400 S5a).

When using 20% data for the independent model validation, MIMICS-T also performs best with the highest accuracy ( $R^2=0.56$ ), the lowest RMSE ( $4.82 \text{ g kg}^{-1}$ ) and the lowest AIC (187.2) among all model versions (Fig. 4, Fig. S5b). MIMICS-TS and MIMICS-TSM<sub>b</sub> have the better correlation ( $R^2=0.52$  and  $0.52$ ), but higher RMSE (RMSE= $5.01 \text{ g kg}^{-1}$  and 405  $5.05 \text{ g kg}^{-1}$ ) and AIC (AIC= $197.7$  and  $198.6$ ) between the observed and simulated cropland SOC concentration than MIMICS-def ( $R^2=0.51$ , RMSE= $4.97 \text{ g kg}^{-1}$ , AIC= $188.8$ ) (Fig. 4e, Fig. S5b).  $R^2$  of the MIMICS-TSM versions ranges from  $0.46$  to  $0.52$ , and  $R^2$  of MIMICS-TSM<sub>b</sub> is highest among them. We also evaluated performances of the MIMICS-TSM<sub>b</sub> version calibrated with cropland SOC data under different crop types. The model performance varies among different crop types (i.e., maize, rice and wheat).  $R^2$  between the simulated SOC concentrations by MIMICS-TSM<sub>b</sub> and observations is higher 410 for maize and wheat ( $0.84$  and  $0.74$ , respectively, Fig. S6a, c) but lowest for rice ( $0.38$ , Fig. S6b). It is probably because the flooded condition in the paddy field limits SOC decomposition, which is partly supported by the weaker correlation between SOC and NPP for rice ( $R^2=0.06$ , Fig. S7d) than that for maize and wheat ( $R^2=0.77$  and  $0.54$ , Fig. S7a, g).

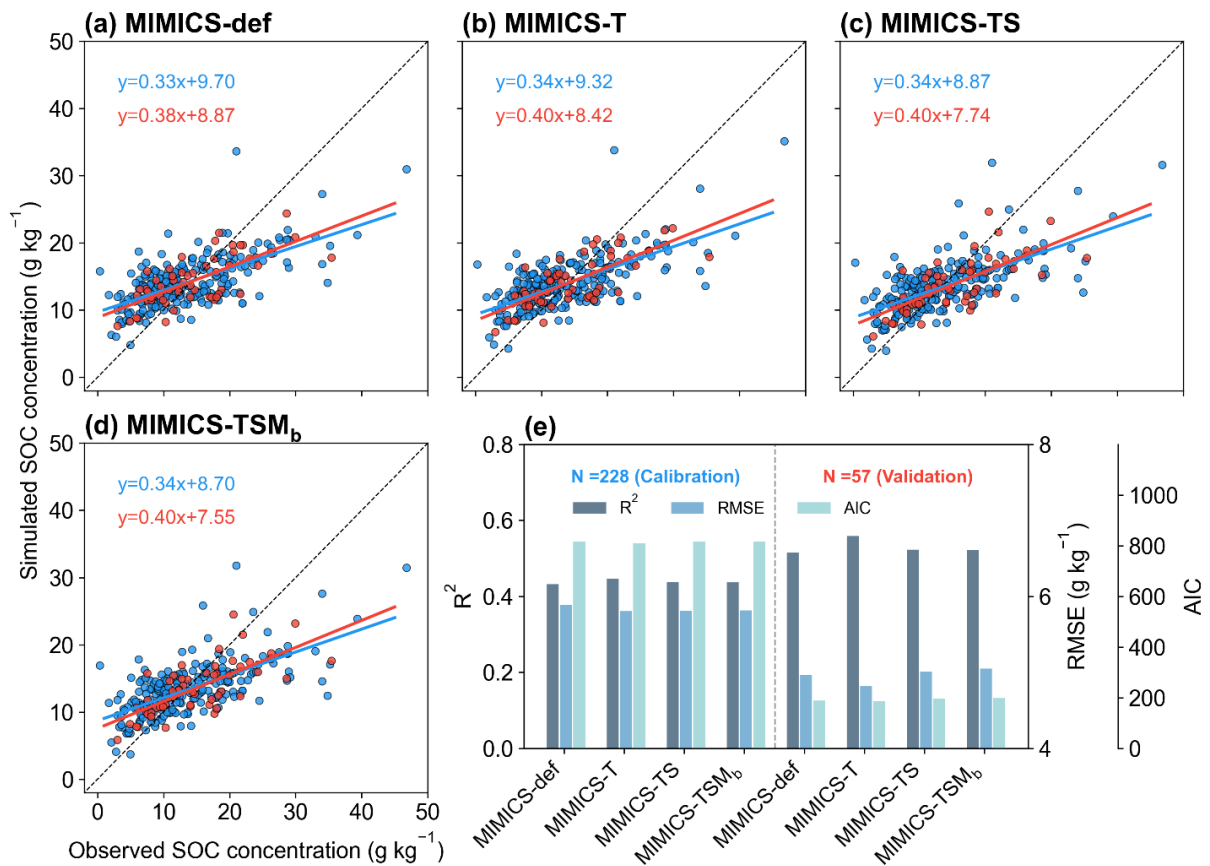


**Fig. 4** Comparison between the observed and simulated SOC concentrations by (a) MIMICS-def, (b) MIMICS-T, (c) 415 MIMICS-TS and (d) MIMICS-TSM<sub>b</sub>. Blue and red dots in (a-d) represent observation sites for model calibration (80% sites)



and validation (20% sites), respectively. (e)  $R^2$ , root mean square error (RMSE) and Akaike information criterion (AIC) from the model calibration (left panel) and validation (right panel) for the four MIMICS versions. Relationships for the other MIMICS versions can be found in Fig. S8.

### 3.1.2 Sensitivity analysis for MIMICS versions without biochar

420 Assuming that the microbial reaction velocity ( $V_{max}$ ) and turnover ( $\tau$ ) were affected by soil moisture, the model with the soil moisture effects does not predict SOC concentrations more accurately ( $R^2=0.46$ ,  $RMSE=5.06 \text{ g kg}^{-1}$ ,  $AIC=198.9$ , Fig. S9b) than the MIMICS-TSM<sub>b</sub> version where  $V_{max}$  and  $K_m$  are affected ( $R^2=0.52$ ,  $RMSE=5.05 \text{ g kg}^{-1}$ ,  $AIC=198.6$ , Fig. 4d, Fig. S5b). In addition, we tested MIMICS after aggregating cropland SOC sites within each  $0.5^\circ \times 0.5^\circ$  grid cell instead of using each site directly, and the model can reproduce about 45%~55% of the SOC spatial variation, slightly lower than that ( $R^2=0.51\sim 0.56$ ,  
 425 Fig.4e) using site-specific data (Fig. S10). The perturbation for input variables of MIMICS shows that the size of steady SOC pool is positively correlated with NPP and Clay, but negatively correlated with MAT and BD. The responses of steady SOC to the perturbation of BD, MAT and NPP are relatively large (Fig. 5).

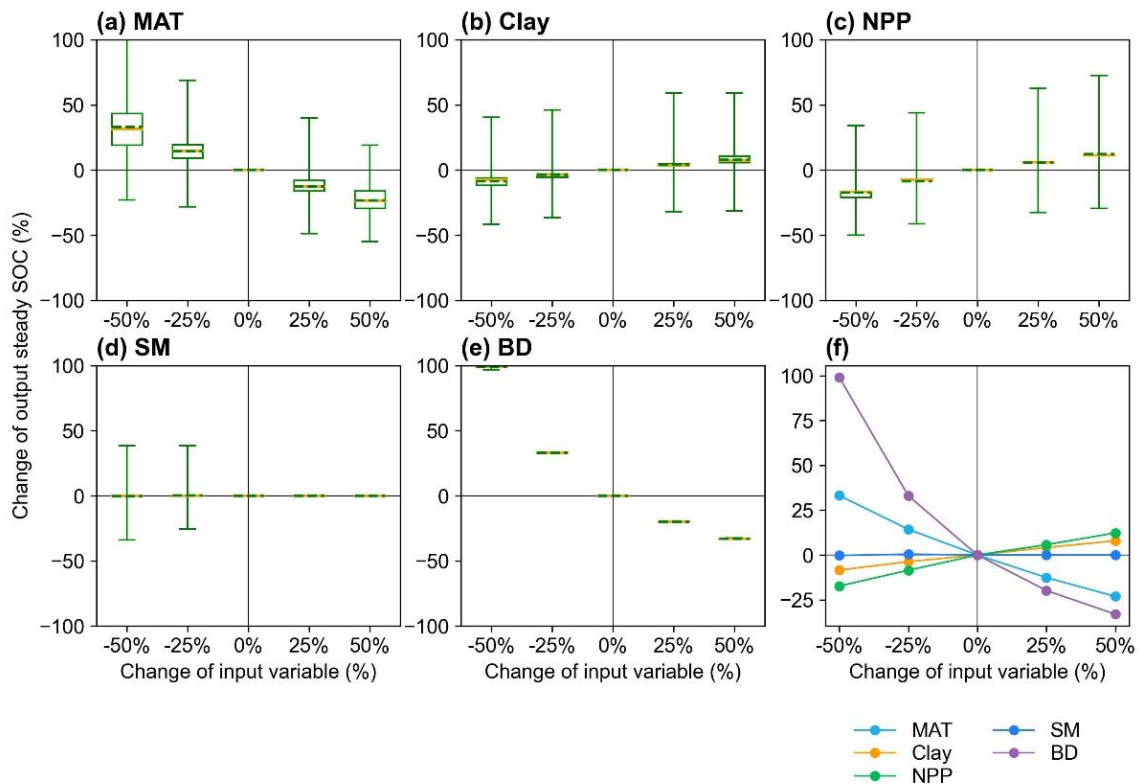


**Fig. 5** Sensitivity analysis of responses of the steady SOC simulated by MIMICS to input variables of (a) MAT, (b) Clay, (c) NPP, (d) SM and (e) BD with different perturbation levels. The yellow line and green dotted line in the boxplot are median and mean values of the output steady SOC changes in calibrated sites. The average SOC changes in calibrated sites for the four perturbation levels are shown in (f).

## 3.2 Calibration and evaluation of MIMICS-BC

### 3.2.1 Calibration and validation for MIMICS-BC versions

435 For the calibration of short-term SOC changes after biochar addition, MIMICS<sub>T-BC</sub> and MIMICS<sub>TSMb-BC</sub> versions with new  
biochar processes show a better performance with higher  $R^2$ , lower RMSE and AIC than MIMICS<sub>T-BC<sub>def</sub></sub> and  
MIMICS<sub>TSMb-BC<sub>def</sub></sub>, respectively (Fig. S11-12). For the model validation using observation data that are not used for  
calibration, the performance of MIMICS<sub>T-BC<sub>DV-SOC<sub>a</sub></sub></sub> ( $R^2=0.80$ , RMSE=3.38 g kg<sup>-1</sup>, AIC=69.8, Fig. 6e-g) is slightly better than  
MIMICS<sub>T-BC<sub>D</sub></sub> ( $R^2=0.79$ , RMSE=3.43 g kg<sup>-1</sup>, AIC=68.5) and MIMICS<sub>T-BC<sub>DV</sub></sub> ( $R^2=0.76$ , RMSE=3.66 g kg<sup>-1</sup>, AIC=74.1),  
440 except for the AIC (69.8) is higher than that of MIMICS<sub>T-BC<sub>D</sub></sub> (68.5) (Fig. 6). By comparison, the performance of  
MIMICS<sub>T-BC<sub>def</sub></sub> is poorer than these three versions. Among the MIMICS<sub>TSMb-BC</sub> versions, MIMICS<sub>TSMb-BC<sub>DV</sub></sub> performs best  
in reproducing SOC changes with biochar addition with the highest  $R^2$  (0.79), the lowest RMSE (3.73 g kg<sup>-1</sup>) and AIC (75.0)  
(Fig. 7e-f). We further calibrated the model at sites with a relatively longer biochar addition period of observations ( $Age_{BC} \geq 3$  yr).  
The corresponding  $R^2$  between observed and simulated SOC changes after biochar addition by MIMICS<sub>TSMb-BC<sub>DV</sub></sub>  
445 (0.20~0.67, Fig. S13c, g, k, o) are lower than that  $R^2$  for all sites (0.63, Fig. S12c, e), except for sites with  $Age_{BC} \geq 3$  yr  
(0.67, Fig. S13c).

For the long-term (extended to 8 yr based on biochar decomposition curve, Wang et al., 2016) SOC changes after biochar  
addition, MIMICS<sub>T-BC<sub>DV</sub></sub> and MIMICS<sub>TSMb-BC<sub>DV</sub></sub> show the best performance among all versions in the model calibration (Fig.  
450 S11-12). In the model validation, MIMICS<sub>T-BC<sub>def</sub></sub> and MIMICS<sub>TSMb-BC<sub>def</sub></sub> underestimate the extrapolated observations of  
SOC change (Fig. 6a, Fig. 7a). MIMICS<sub>T-BC<sub>D</sub></sub> shows the best performance with the lowest RMSE (3.84 g kg<sup>-1</sup>) and AIC (74.7)  
among all the MIMICS<sub>T-BC</sub> versions (Fig. 6). Compared to MIMICS<sub>TSMb-BC<sub>def</sub></sub> ( $R^2=0.88$ , RMSE=9.35 g kg<sup>-1</sup>, slope=0.08,  
AIC=120.7, Fig. 7a, e, f, g), predictions of MIMICS<sub>TSMb-BC<sub>D</sub></sub>, MIMICS<sub>TSMb-BC<sub>DV</sub></sub> and MIMICS<sub>TSMb-BC<sub>DV-SOC<sub>a</sub></sub></sub> are more  
accurate with a smaller RMSE (8.12 g kg<sup>-1</sup>, 6.08 g kg<sup>-1</sup> and 6.78 g kg<sup>-1</sup>, Fig. 7f), a smaller AIC (115.1, 101.5 and 107.4, Fig. 7g),  
455 a linear slope closer to 1 (0.29, 1.68 and 1.74, Fig. 7a-d), and a reasonable accuracy of  $R^2$  (0.45, 0.97 and 0.94, Fig. 7e). Among  
the different MIMICS<sub>TSMb-BC</sub> versions, MIMICS<sub>TSMb-BC<sub>DV</sub></sub> shows the best performance (Fig. 7). When assuming that  
biochar produces a priming effect only through affecting the utilization rate of SOC<sub>a</sub> by microbes (MIMICS<sub>TSMb-BC<sub>DV-SOC<sub>a</sub></sub></sub>),  
the model accuracy is slightly decreased with lower  $R^2$  (=0.94), higher RMSE (=6.78 g kg<sup>-1</sup>) and higher AIC (=107.4) than  
MIMICS<sub>TSMb-BC<sub>DV</sub></sub> that assumes all decomposition processes are affected (Fig. 7).

460

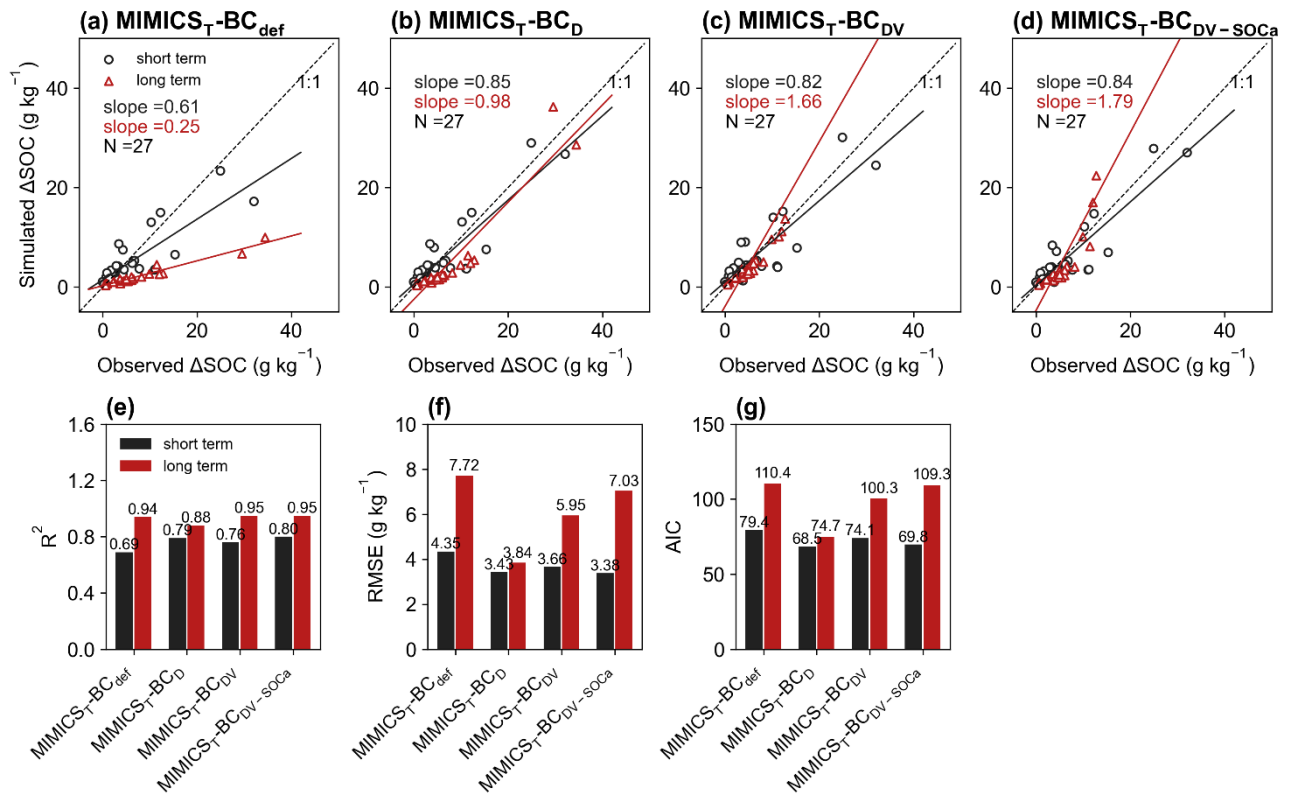


**Fig. 6** Relationships of short-term ( $\leq 6$  yr; black) and long-term (i.e., extended to 8 yr; red) SOC changes after biochar addition ( $\Delta$ SOC) between observations and models in validation dataset. The MIMICS versions are used, including MIMICS<sub>T</sub>-BC<sub>def</sub> (a), MIMICS<sub>T</sub>-BC<sub>D</sub> (b), MIMICS<sub>T</sub>-BC<sub>DV</sub> (c) and MIMICS<sub>T</sub>-BC<sub>DV-SOCa</sub> (d). Comparisons of R<sup>2</sup> (e), the root mean square error (RMSE, f) and the Akaike information criterion (AIC, g) among the four MIMICS<sub>T</sub>-BC versions are shown separately. See model versions in Table 1.

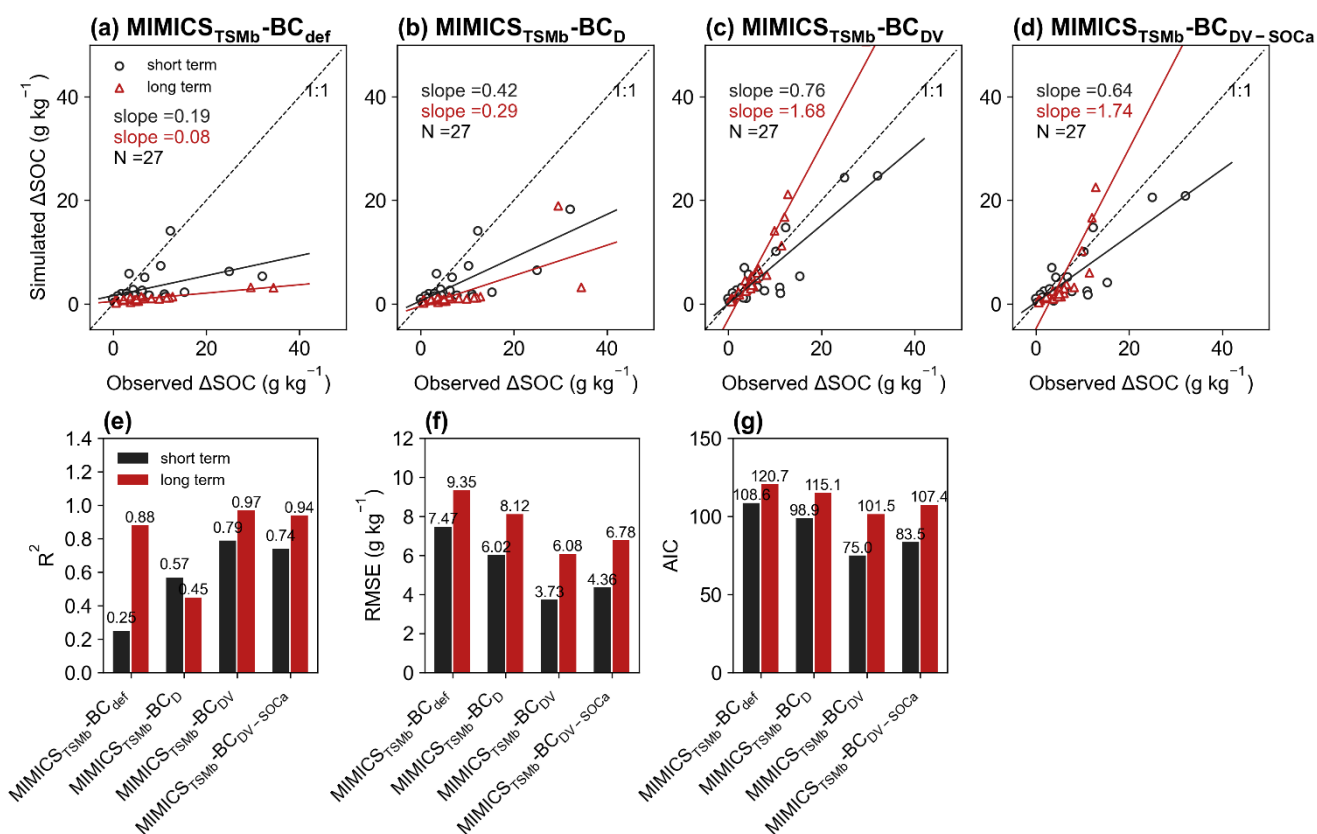
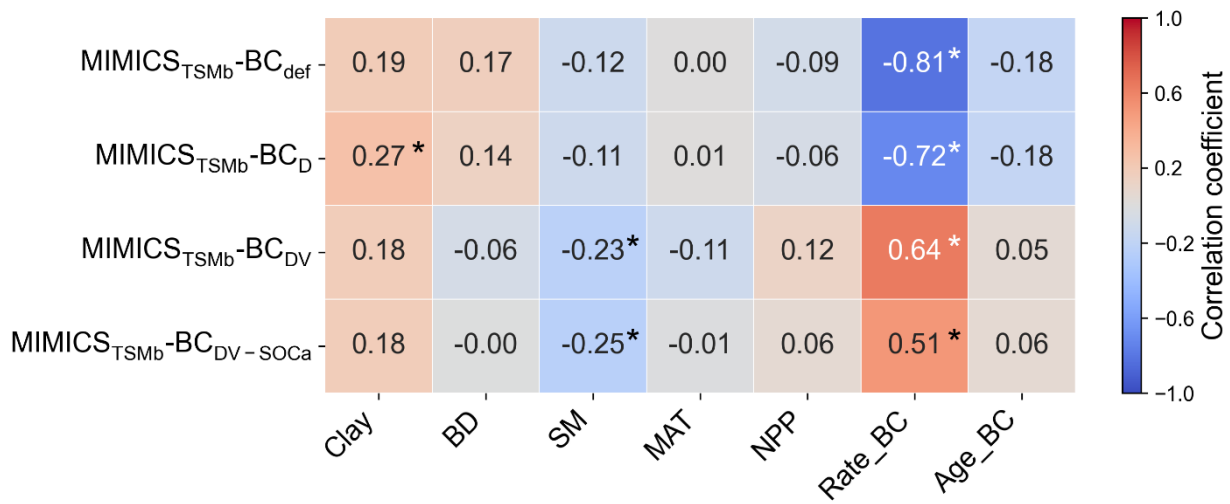


**Fig. 7** Relationships of short-term ( $\leq 6$  yr; black) and long-term (i.e., extended to 8 yr; red) SOC changes after biochar addition ( $\Delta$ SOC) between observations and models in validation dataset. The MIMICS versions are used, including  
 470 MIMICS<sub>TSMb-BC<sub>def</sub></sub> (a), MIMICS<sub>TSMb-BC<sub>D</sub></sub> (b), MIMICS<sub>TSMb-BC<sub>DV</sub></sub> (c) and MIMICS<sub>TSMb-BC<sub>DV-SOCa</sub></sub> (d). Comparisons of R<sup>2</sup> (e), the root mean square error (RMSE, f) and the Akaike information criterion (AIC, g) among the four MIMICS<sub>TSMb-BC</sub> versions are shown separately. See model versions in Table 1.

### 3.2.2 Error analysis for MIMICS-BC versions

The biases between the simulated and observed short-term SOC changes with biochar addition are significantly correlated  
 475 with Rate<sub>BC</sub> or Clay ( $p < 0.05$ ), but only vary marginally with SM, MAT and NPP when additional parameters are optimized (Fig. S14). The biases between long-term observations and simulations by MIMICS<sub>TSMb-BC<sub>def</sub></sub> are significantly correlated with Rate<sub>BC</sub> ( $r = -0.81$ ) (Fig. 8), suggesting that the model may underrepresent processes related to Rate<sub>BC</sub>. By considering biochar effects on the SOC desorption (MIMICS<sub>TSMb-BC<sub>D</sub></sub>), the correlations of model biases with Rate<sub>BC</sub>, BD, SM and NPP become weaker (Fig. 8). MIMICS<sub>TSMb-BC<sub>DV</sub></sub> incorporating the biochar impacts on microbial decomposition rate  
 480 further reduces the correlations between model biases and variables of Rate<sub>BC</sub>, Age<sub>BC</sub> and BD. MIMICS<sub>TSMb-BC<sub>DV-SOCa</sub></sub> including the impacts on microbial decomposition rate only in the fluxes from SOC<sub>a</sub> to MIC pools can also reduce the correlations between model biases and variables of Rate<sub>BC</sub> and BD, but the correlations change little with Clay and Age<sub>BC</sub> (Fig. 8).



485 **Fig. 8** Correlations between the MIMICS<sub>TSMb</sub>-BC biases (i.e., simulated long-term  $\Delta$ SOC minus observed  $\Delta$ SOC) and input soil- (Clay, BD, SM), climate- (MAT), biological- (NPP) and biochar-related (Rate\_BC, Age\_BC) variables for MIMICS<sub>TSMb</sub>-BC<sub>def</sub>, MIMICS<sub>TSMb</sub>-BC<sub>D</sub>, MIMICS<sub>TSMb</sub>-BC<sub>DV</sub> and MIMICS<sub>TSMb</sub>-BC<sub>DV-SOCa</sub>. Asterisks indicate significant correlations ( $p < 0.05$ ).

### 3.2.3 Sensitivity analysis for MIMICS-BC versions

490 The test of the partitioning coefficient from biochar to SOC<sub>a</sub> ( $f_{ba}$ ) with 2% for the MIMICS<sub>TSMb</sub>-BC model (see **Section 2.3.3**) shows a similar  $R^2$  (0.35~0.79, Fig. S15) to that from  $f_{ba} = 20\%$  in short-term (0.25~0.79, Fig. 7). The optimization (MIMICS<sub>TSMb</sub>-BC<sub>DV\*</sub>) of the partitioning coefficient from biochar carbon to SOC<sub>p</sub> ( $f_{bp}$ ) and  $f_{ba}$  shows a better performance ( $R^2=0.80$ , RMSE=3.44 g kg<sup>-1</sup>, AIC=66.7, Fig. S16) than MIMICS<sub>TSMb</sub>-BC<sub>DV</sub> that without these two parameters optimized. The responses of  $\Delta$ SOC to parameter perturbations show that  $f_v$  and  $f_d$  affect  $\Delta$ SOC with biochar addition in the opposite directions,

495 and  $\Delta$ SOC is more sensitive to the partition coefficient  $f_{bp}$  than  $f_d$ ,  $f_v$  and  $f_{ba}$  (Fig. 9).  $\Delta$ SOC is more sensitive to Rate\_BC than Age\_BC. The sensitivity of the  $\Delta$ SOC to  $\tau$  is greater than that to MGE (Fig. S17), and the two parameters may be influenced by biochar but are not considered in the current MIMICS-BC versions. The sensitivity tests for the model input variables, i.e., crop net primary productivity (NPP), soil clay content (Clay) and soil moisture (SM), show that Clay is very important to the model outputs, while the impacts of NPP and SM are relatively smaller (Fig. S17).

500

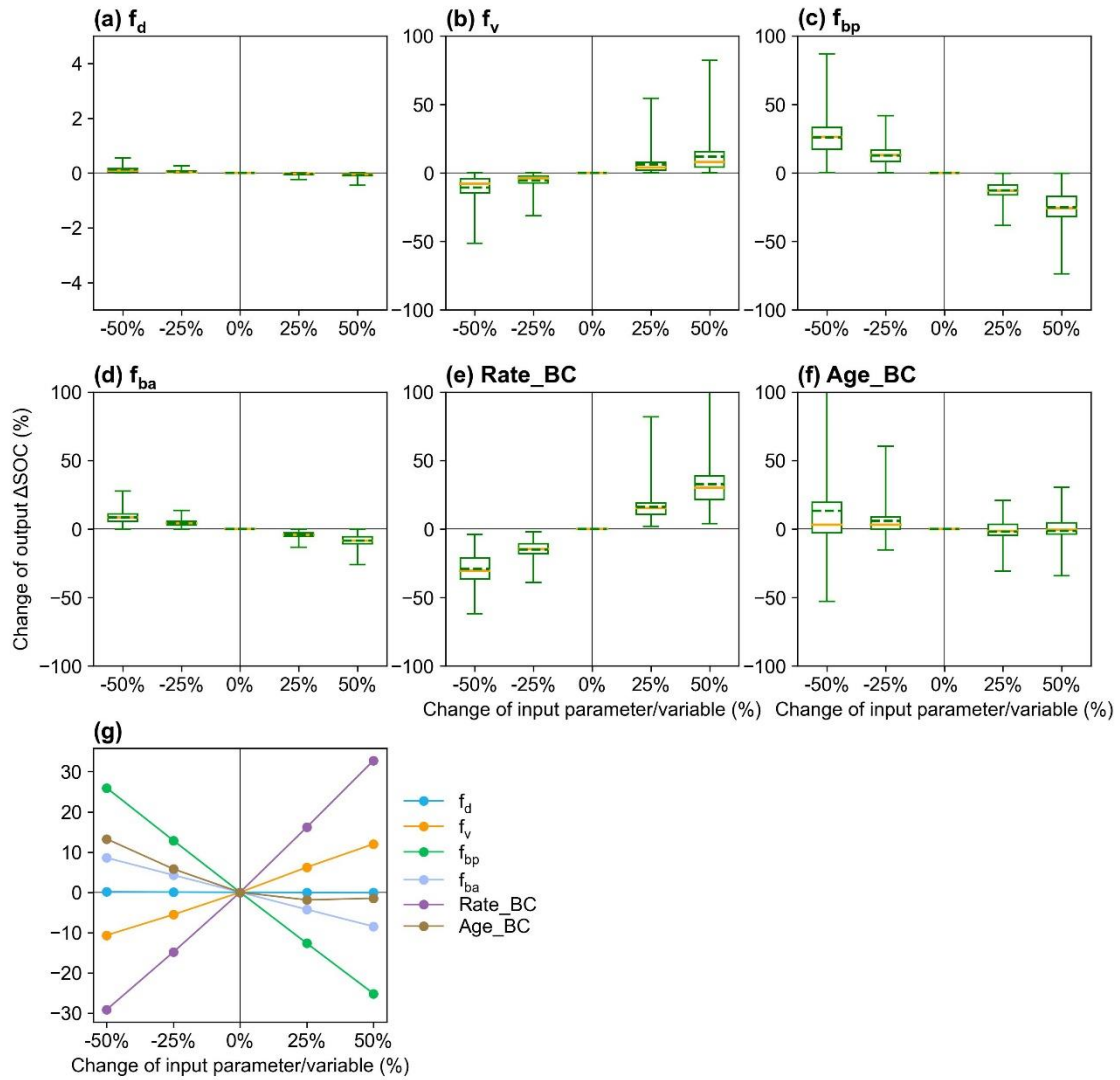


**Fig. 9** Sensitivity analysis of MIMICS-BC model parameters of (a)  $f_d$  (desorption coefficient, Eq. 15), (b)  $f_v$  (decomposition rate coefficient, Eq. 16), (c)  $f_{bp}$  (partition coefficient from biochar carbon to  $\text{SOC}_p$ , Fig. 1), (d)  $f_{ba}$  (partition coefficient from biochar carbon to  $\text{SOC}_a$ , Fig. 1), and the biochar-related input variables of (e) Rate\_BC and (f) Age\_BC. The yellow line and  
 505 green dotted line in boxplots are median and mean values of the changes in model output (i.e., change of  $\Delta$ SOC, Eq. 19). The mean values of change of output  $\Delta$ SOC in calibrated sites are shown in (g).

## 4. Discussion

### 4.1 Cropland SOC related processes

#### 4.1.1 Missing processes in the MIMICS model

510 We presented a framework to quantify the impact of microbial density-dependent turnover, sorption, and soil moisture effects on cropland SOC dynamics. Regulatory mechanisms (e.g., competition) may limit microbial population sizes, and neglecting this process could lead to indefinite microbial biomass growth with increasing litter inputs (Georgiou et al., 2017).

Our analysis demonstrates that restricting microbial biomass size through density-dependent microbial turnover (MIMICS-T) slightly improves the model performance (Fig. 4), but further including sorption and soil moisture effects (MIMICS-TS and MIMICS-TSM) has negligible contribution to the model performance. One possible reason is that the inclusion of these new processes greatly increases model complexity, but in the parameter calibrations, SOC is still the only observational variable to constrain all the newly added processes. Therefore, the model parameters may not be fully constrained due to the lack of direct observations on these new processes.

Another reason is that some other possibly important processes are missing from the model. For example, the MIMICS-TS version considers the impacts of soil clay on the adsorption capacity of SOC<sub>a</sub>, but soil pH, ionic strength and mineral content are also found important to the sorption-desorption of SOC (Kothawala et al., 2009; Mayes et al., 2012). The metal ion Ca<sup>2+</sup> can form bonds between negatively charged clay minerals and available SOC via cation bridging, enhancing the adsorption of available SOC by soil clay minerals (Roychand and Marschner, 2014; Setia et al., 2013). Soil pH can also impact SOC sorption by altering the ionization degree and the surface charge of SOC molecules (Shen., 1999). Moreover, the iron minerals can preferentially bind to lignin components through sorption and coprecipitation, protecting it from microbial degradation and consequently increasing SOC (Liao et al., 2022). In addition to the sorption-desorption process that is associated with microbial accessibility to SOC, other factors that influence microbial activity are also underrepresented in MIMICS, such as the soil nutrient availability (e.g., nitrogen), which greatly impacts microbial use efficiency and growth rate (Manzoni et al., 2017). These processes improve our understanding of the mechanisms of SOC dynamics and should be incorporated in the model to represent the microbial-mineral processes realistically and mechanistically.

However, as shown in our results, without further observational constraints on each process separately, the model performance only relying on calibrations against total SOC contents may not improve. Therefore, various versions of MIMICS, representing different levels of our understanding on microbial-mineral processes, are retained in our study for further calibrations when sufficient observations emerge.

#### **4.1.2 Cropland management impacts**

Cropland management disturbs soils frequently, and the assumed equilibrium state of SOC may not be realistic, which also partly explains the mismatch between simulated and observed SOC. Agriculture management (e.g., irrigation, tillage) are important factors that affect SOC decomposition and accumulation in croplands. The poor performance of MIMICS for rice is probably due to inability of MIMICS to simulate SOC dynamics under anaerobic condition from the irrigation practice (Fig. S6-7). Tillage may disrupt soil aggregates and release physically protected SOC, which is more susceptible to decomposition than that protected by soil aggregates (Six et al., 1999). Juice et al. (2022) modeled tillage effects on SOC loss through

transferring protected SOC into unprotected pools, i.e., from  $SOC_p$  to  $SOC_a$  in this study. Our results from variable perturbation  
545 suggest that the BD is the key driver to SOC changes, followed by MAT and crop NPP (Fig. 5), suggesting that processes  
related to these variables have a great effect on the SOC. The soil BD was also found to be affected by tillage practices  
(Osunbitan et al., 2005), and crop NPP may vary due to crop rotation and fallow practice, which are missing in the model.

In addition, managements such as fertilizer application and possible residue retention can increase SOC stock. Previous  
550 evidence indicates that the SOC is increased by 11.3% with residue return (Wang et al., 2020b) and by 13.3% with straw  
return and balanced NPK fertilizer (Islam et al., 2023) compared to residue removal. However, these management processes  
of fertilization and residue retention are not represented in the MIMICS model due to the absence of quantitative  
management data and the poor understanding of the mechanisms. It may explain the underestimation of SOC at sites with a  
high carbon density by the calibrated MIMICS models (Fig. 4). Therefore, field measurements on the effects of agricultural  
555 practices on SOC dynamic are urgently needed to further improve the model processes (Campbell et al., 2007; Congreves et  
al., 2015).

## 4.2 Biochar-related processes

### 4.2.1 Tested processes in the MIMICS-BC model

Biochar can absorb SOC due to its large specific surface area, high porosity and further promotion of soil macro-aggregates  
560 formation (Han et al., 2020; Huang et al., 2018). Consistently, the optimized desorption coefficient ( $f_d = -0.0121$  and  $-0.0122$   
for short- and long-term, Table S3) in  $MIMICS_{TSMb-BCD}$  is negative, indicating the carbon desorption from  $SOC_p$  to  $SOC_a$  is  
reduced with biochar addition. Incorporating the biochar impacts on microbial decomposition velocity in the  
 $MIMICS_{TSMb-BCDV}$  further improved model with biochar addition, but the correlations between model-observation biases and  
input variables of biochar application rate (Rate\_BC) and soil moisture (SM) are still significant in long term ( $p < 0.05$ , Fig. 8),  
565 implying that some processes related to these variables are not well represented in the model. For example, biochar addition  
could increase soil moisture (Razzaghi et al. 2020), and further alter the composition and activities of soil microbial  
communities (Lehmann et al. 2011). Moreover, the direction and magnitude of biochar effects on SOC are dependent on  
biochar addition rate and incubation times (Ding et al., 2017). Compared to  $MIMICS_{T-BCDV}$ ,  $MIMICS_{T-BCDV-SOCa}$  performed  
better in the short-term SOC response to biochar addition but worse in the long-term response (Fig. 6). When biochar is applied,  
570 the labile carbon fraction may be immediately utilized by microbes, and thus adding biochar effects on the  $SOC_a$  process is  
important for the short-term response. In the long term, the SOC mineralization may be gradually suppressed via physical  
protection (Zimmerman et al., 2011), but both  $MIMICS_{T-BCDV}$  and  $MIMICS_{T-BCDV-SOCa}$  do not include the adsorption process.  
In the  $MIMICS_{TSMb-BC}$  versions that include the adsorption process, the available SOC may be partly adsorbed by soil



minerals and become physically protected. This could lead to the positive priming effect of biochar on SOC being less  
575 evident (Fig. 7).

#### 4.2.2 Missing processes in current MIMICS-BC model

The effects of biochar on SOC are controlled by various factors, such as soil physicochemical and biological properties (e.g.,  
clay, pH, microbial activity), biochar properties (e.g., feedstock, pyrolysis temperature) and incubation conditions (e.g.,  
periods, crop types) (Ding et al., 2017; Han et al., 2020). Some of these effects are not explicitly considered in the MIMICS  
580 biochar version. Biochar addition may change the composition of microbial community, and a previous study reported  
increased copiotrophic bacteria with a higher growth rate and decreased oligotrophic bacteria in acid soils with biochar  
addition (Sheng and Zhu, 2018). This is related to the competition between r- and k-strategy microbes in MIMICS. Microbial  
carbon use efficiency (CUE) determines the relation proportions of microbial carbon uptake between growth and respiration  
(Zhou et al., 2017a), and increased CUE and reduced turnover time ( $1/\tau$ ) of microbial biomass were found with biochar  
585 addition, although the changes depend on the soil texture (Pei et al., 2021). It is consistent with our results that the  $\Delta$ SOC is  
more sensitive to changes of  $\tau$  and soil clay than other parameters and variables (Fig. S17). Therefore, processes and  
parameters related to  $\tau$  and soil clay need to be accounted for in future with additional evidence.

In the MIMICS-BC version, we assumed that biochar, with a longer turnover time (about 1000 yr, Schmidt et al., 2002) than  
590 SOC, are evenly mixed with SOC and are treated as a homogenous pool without an explicit vertical profile, which may also  
bring uncertainties. In addition, due to lack of long-term biochar addition experiments, the extended long-term SOC  
concentrations with biochar addition are calculated as the sum of SOC in the control site without biochar addition and the  
remaining biochar carbon based on the biochar degradation curve (Fig. S4; Wang et al., 2016). Although they are not direct  
observations and may induce uncertainty, the long-term model validation is important to assess the model ability of simulating  
595 the SOC stability with biochar addition. Long-term and comprehensive field measurements of SOC and other soil and microbe  
properties after biochar addition are therefore urgently needed to understand the underlying mechanisms of biochar impacts on  
SOC changes, all of which will help improve the model performance.

## 5. Conclusion

Our study shows that the updated MIMICS versions with new processes (e.g., adsorption and soil moisture) improves the  
600 model performance on simulating SOC dynamics on croplands. The model versions implemented with biochar processes can  
generally capture the SOC changes after biochar application from observations. Biochar is believed to have a large CDR  
potential, and its application on soils would affect the soil carbon and nutrient cycles. These impacts need to be incorporated  
ESMs to accurately simulate the mitigation potential of biochar under future climate change.

**Code availability.** The codes of this model version are available at <https://doi.org/10.5281/zenodo.8112967> (Han et al., 605 2023).

**Author contributions.** Mengjie Han collected the site measurements data for model evaluation, performed the simulations and optimized the model code, and prepared the manuscript. Qing Zhao and Wei Li conceived the study and designed the experiments. Wei Li, Ying-Ping Wang, Philippe Ciais, Haicheng Zhang, Daniel S. Goll, Chen Wang and Wei Zhuang guided and improved the manuscript in technology, logic and detail. Lei Zhu, Zhe Zhao and Zhixuan Guo assisted with the technical 610 aspects in data acquisition and analysis. Xili Wang and Fengchang Wu reviewed and revised the manuscript.

**Competing interests.** The authors declare that they have no conflict of interest.

**Acknowledgements.** This study was funded by the Yunnan Provincial Science and Technology Project at Southwest United Graduate School (grant number: 202302AO370001), the National Natural Science Foundation of China (grant number: 42192574, 42022056, 42175169) and Tsinghua University Initiative Scientific Research Program (grant number: 615 20223080041).

## References

- Abiven, S., Recous, S., Reyes, V., and Oliver, R.: Mineralisation of C and N from root, stem and leaf residues in soil and role of their biochemical quality, *Biology and Fertility of Soils*, 42, 119-128, 10.1007/s00374-005-0006-0, 2005.
- 620 Abramoff, R. Z., Guenet, B., Zhang, H., Georgiou, K., Xu, X., Rossel, R. A. V., Yuan, W., and Ciais, P.: Improved global-scale predictions of soil carbon stocks with Millennial Version 2, *Soil Biology and Biochemistry*, 164, 108466, 2022.
- Akaike, H.: A new look at the statistical model identification, *IEEE transactions on automatic control*, 19, 716-723, 1974.
- Allison, S. D., Wallenstein, M. D., and Bradford, M. A.: Soil-carbon response to warming dependent on microbial 625 physiology, *Nature Geoscience*, 3, 336-340, 10.1038/ngeo846, 2010.
- Archontoulis, S. V., Huber, I., Miguez, F. E., Thorburn, P. J., Rogovska, N., and Laird, D. A.: A model for mechanistic and system assessments of biochar effects on soils and crops and trade - offs, *GCB Bioenergy*, 8, 1028-1045, 10.1111/gcbb.12314, 2016.
- Bond-Lamberty, B., Bailey, V. L., Chen, M., Gough, C. M., and Vargas, R.: Globally rising soil heterotrophic respiration 630 over recent decades, *Nature*, 560, 80-83, 10.1038/s41586-018-0358-x, 2018.
- Buchkowski, R. W., Bradford, M. A., Grandy, A. S., Schmitz, O. J., and Wieder, W. R.: Applying population and community ecology theory to advance understanding of belowground biogeochemistry, *Ecol Lett*, 20, 231-245, 10.1111/ele.12712, 2017.
- Camino-Serrano, M., Guenet, B., Luysaert, S., Ciais, P., Bastrikov, V., De Vos, B., Gielen, B., Gleixner, G., Jornet-Puig, A., 635 Kaiser, K., Kothawala, D., Lauerwald, R., Peñuelas, J., Schrumpf, M., Vicca, S., Vuichard, N., Walmsley, D., and Janssens, I. A.: ORCHIDEE-SOM: modeling soil organic carbon (SOC) and dissolved organic carbon (DOC) dynamics along vertical soil profiles in Europe, *Geoscientific Model Development*, 11, 937-957, 10.5194/gmd-11-937-2018, 2018.
- Campbell, C. A., VandenBygaart, A. J., Zentner, R. P., McConkey, B. G., Smith, W., Lemke, R., Grant, B., and Jefferson, P. 640 G.: Quantifying carbon sequestration in a minimum tillage crop rotation study in semiarid southwestern Saskatchewan, *Canadian Journal of Soil Science*, 87, 235-250, 10.4141/s06-018, 2007.
- Congreves, K. A., Grant, B. B., Campbell, C. A., Smith, W. N., VandenBygaart, A. J., Kröbel, R., Lemke, R. L., and Desjardins, R. L.: Measuring and Modeling the Long - Term Impact of Crop Management on Soil Carbon

- Sequestration in the Semiarid Canadian Prairies, *Agronomy Journal*, 107, 1141-1154, 10.2134/agronj15.0009, 2015.
- 645 Ding, F., Van Zwieten, L., Zhang, W., Weng, Z., Shi, S., Wang, J., and Meng, J.: A meta-analysis and critical evaluation of influencing factors on soil carbon priming following biochar amendment, *Journal of Soils and Sediments*, 18, 1507-1517, 10.1007/s11368-017-1899-6, 2017.
- Duan, Q. Y., Sorooshian, S., and Gupta, V. K.: Optimal use of the SCE-UA global optimization method for calibrating watershed models, *Journal of Hydrology*, 158, 265-284, 10.1016/0022-1694(94)90057-4, 1994.
- 650 Eglin, T., Ciais, P., Piao, S. L., Barre, P., Bellassen, V., Cadule, P., Chenu, C., Gasser, T., Koven, C., Reichstein, M., and Smith, P.: Historical and future perspectives of global soil carbon response to climate and land-use changes, *Tellus B: Chemical and Physical Meteorology*, 62, 700-718, 10.1111/j.1600-0889.2010.00499.x, 2010.
- El-Naggar, A., El-Naggar, A. H., Shaheen, S. M., Sarkar, B., Chang, S. X., Tsang, D. C. W., Rinklebe, J., and Ok, Y. S.: Biochar composition-dependent impacts on soil nutrient release, carbon mineralization, and potential environmental risk: A review, *J Environ Manage*, 241, 458-467, 10.1016/j.jenvman.2019.02.044, 2019.
- 655 Entekhabi, D., Njoku, E. G., O'Neill, P. E., Kellogg, K. H., Crow, W. T., Edelstein, W. N., Entin, J. K., Goodman, S. D., Jackson, T. J., Johnson, J., Kimball, J., Piepmeier, J. R., Koster, R. D., Martin, N., McDonald, K. C., Moghaddam, M., Moran, S., Reichle, R., Shi, J. C., Spencer, M. W., Thurman, S. W., Tsang, L., and Van Zyl, J.: The Soil Moisture Active Passive (SMAP) Mission, *Proceedings of the IEEE*, 98, 704-716, 10.1109/jproc.2010.2043918, 2010.
- 660 Fick, S. E. and Hijmans, R. J.: WorldClim 2: new 1 - km spatial resolution climate surfaces for global land areas, *International Journal of Climatology*, 37, 4302-4315, 10.1002/joc.5086, 2017.
- Fuss, S., Lamb, W. F., Callaghan, M. W., Hilaire, J., Creutzig, F., Amann, T., Beringer, T., de Oliveira Garcia, W., Hartmann, J., Khanna, T., Luderer, G., Nemet, G. F., Rogelj, J., Smith, P., Vicente, J. L. V., Wilcox, J., del Mar Zamora Dominguez, M., and Minx, J. C.: Negative emissions—Part 2: Costs, potentials and side effects, *Environmental Research Letters*, 13, 10.1088/1748-9326/aabf9f, 2018.
- 665 Geisseler, D., Linqvist, B. A., and Lazicki, P. A.: Effect of fertilization on soil microorganisms in paddy rice systems – A meta-analysis, *Soil Biology and Biochemistry*, 115, 452-460, 10.1016/j.soilbio.2017.09.018, 2017.
- Georgiou, K., Abramoff, R. Z., Harte, J., Riley, W. J., and Torn, M. S.: Microbial community-level regulation explains soil carbon responses to long-term litter manipulations, *Nat Commun*, 8, 1223, 10.1038/s41467-017-01116-z, 2017.
- 670 Han, L., Sun, K., Yang, Y., Xia, X., Li, F., Yang, Z., and Xing, B.: Biochar's stability and effect on the content, composition and turnover of soil organic carbon, *Geoderma*, 364, 10.1016/j.geoderma.2020.114184, 2020.
- Han, M., Zhao, Q., Li, W., Ciais, P., Wang, Y. P., Goll, D. S., Zhu, L., Zhao, Z., Wang, J., Wei, Y., and Wu, F.: Global soil organic carbon changes and economic revenues with biochar application, *GCB Bioenergy*, 14, 364-377, 10.1111/gcbb.12915, 2021.
- 675 Harris, I., Jones, P. D., Osborn, T. J., and Lister, D. H.: Updated high-resolution grids of monthly climatic observations - the CRU TS3.10 Dataset, *International Journal of Climatology*, 34, 623-642, 10.1002/joc.3711, 2014.
- Hicke, J. A. and Lobell, D. B.: Spatiotemporal patterns of cropland area and net primary production in the central United States estimated from USDA agricultural information, *Geophysical Research Letters*, 31, 2004.
- Houska, T., Kraft, P., Chamorro-Chavez, A., and Breuer, L.: SPOTting Model Parameters Using a Ready-Made Python 680 Package, *PLoS One*, 10, e0145180, 10.1371/journal.pone.0145180, 2015.
- Huang, R., Tian, D., Liu, J., Lv, S., He, X., and Gao, M.: Responses of soil carbon pool and soil aggregates associated organic carbon to straw and straw-derived biochar addition in a dryland cropping mesocosm system, *Agriculture, Ecosystems & Environment*, 265, 576-586, 10.1016/j.agee.2018.07.013, 2018.
- Islam, M. U., Jiang, F., Halder, M., Liu, S., and Peng, X.: Impact of straw return combined with different fertilizations on soil organic carbon stock in upland wheat and maize croplands in China: A meta-analysis, *Crop and Environment*, 2, 233-241, 2023.
- 685 Jansson, J. K. and Wu, R.: Soil viral diversity, ecology and climate change, *Nature Reviews Microbiology*, 21, 296-311, 10.1038/s41579-022-00811-z, 2023.
- Juice, S. M., Walter, C. A., Allen, K. E., Berardi, D. M., Hudiburg, T. W., Sulman, B. N., and Brzostek, E. R.: A new 690 bioenergy model that simulates the impacts of plant - microbial interactions, soil carbon protection, and mechanistic

- tillage on soil carbon cycling, *GCB Bioenergy*, 14, 346-363, 10.1111/gcbb.12914, 2022.
- Kalbitz, K., Schwesig, D., Rethemeyer, J., and Matzner, E.: Stabilization of dissolved organic matter by sorption to the mineral soil, *Soil Biology and Biochemistry*, 37, 1319-1331, 10.1016/j.soilbio.2004.11.028, 2005.
- 695 Kasozi, G. N., Zimmerman, A. R., Nkedi-Kizza, P., and Gao, B.: Catechol and humic acid sorption onto a range of laboratory-produced black carbons (biochars), *Environmental science & technology*, 44, 6189-6195, 2010.
- Kobayashi, S., Ota, Y., Harada, Y., Ebita, A., Moriya, M., Onoda, H., Onogi, K., Kamahori, H., Kobayashi, C., Endo, H., Miyaoka, K., and Takahashi, K.: The JRA-55 Reanalysis: General Specifications and Basic Characteristics, *Journal of the Meteorological Society of Japan. Ser. II*, 93, 5-48, 10.2151/jmsj.2015-001, 2015.
- 700 Kothawala, D., Moore, T., and Hendershot, W.: Soil properties controlling the adsorption of dissolved organic carbon to mineral soils, *Soil Science Society of America Journal*, 73, 1831-1842, 2009.
- Kyker-Snowman, E., Wieder, W. R., Frey, S. D., and Grandy, A. S.: Stoichiometrically coupled carbon and nitrogen cycling in the MInicrobial-MIneral Carbon Stabilization model version 1.0 (MIMICS-CN v1. 0), *Geoscientific Model Development*, 13, 4413-4434, 2020.
- Lehmann, J., Rillig, M. C., Thies, J., Masiello, C. A., Hockaday, W. C., and Crowley, D.: Biochar effects on soil biota – A 705 review, *Soil Biology and Biochemistry*, 43, 1812-1836, 10.1016/j.soilbio.2011.04.022, 2011.
- Lehmann, J., Cowie, A., Masiello, C. A., Kammann, C., Woolf, D., Amonette, J. E., Cayuela, M. L., Camps-Arbestain, M., and Whitman, T.: Biochar in climate change mitigation, *Nature Geoscience*, 14, 883-892, 10.1038/s41561-021-00852-8, 2021.
- Li, Z., Song, Z., Singh, B. P., and Wang, H.: The impact of crop residue biochars on silicon and nutrient cycles in croplands, 710 *Sci Total Environ*, 659, 673-680, 10.1016/j.scitotenv.2018.12.381, 2019.
- Liang, J., Wang, G., Ricciuto, D. M., Gu, L., Hanson, P. J., Wood, J. D., and Mayes, M. A.: Evaluating the E3SM land model version 0 (ELMv0) at a temperate forest site using flux and soil water measurements, *Geoscientific Model Development*, 12, 1601-1612, 10.5194/gmd-12-1601-2019, 2019.
- Liao, C., Huang, W., Wells, J., Zhao, R., Allen, K., Hou, E., Huang, X., Qiu, H., Tao, F., Jiang, L., Aguilos, M., Lin, L., 715 Huang, X., and Luo, Y.: Microbe-iron interactions control lignin decomposition in soil, *Soil Biology & Biochemistry*, 173, 10.1016/j.soilbio.2022.108803, 2022.
- Luo, Y., Durenkamp, M., De Nobili, M., Lin, Q., and Brookes, P. C.: Short term soil priming effects and the mineralisation of biochar following its incorporation to soils of different pH, *Soil Biology and Biochemistry*, 43, 2304-2314, 10.1016/j.soilbio.2011.07.020, 2011.
- 720 Luo, Y., Zang, H., Yu, Z., Chen, Z., Gunina, A., Kuzyakov, Y., Xu, J., Zhang, K., and Brookes, P. C.: Priming effects in biochar enriched soils using a three-source-partitioning approach: <sup>14</sup>C labelling and <sup>13</sup>C natural abundance, *Soil Biology and Biochemistry*, 106, 28-35, 2017.
- Lychuk, T. E., Izaurrealde, R. C., Hill, R. L., McGill, W. B., and Williams, J. R.: Biochar as a global change adaptation: predicting biochar impacts on crop productivity and soil quality for a tropical soil with the Environmental Policy 725 Integrated Climate (EPIC) model, *Mitigation and Adaptation Strategies for Global Change*, 20, 1437-1458, 10.1007/s11027-014-9554-7, 2014.
- Manzoni, S. and Porporato, A.: Soil carbon and nitrogen mineralization: Theory and models across scales, *Soil Biology and Biochemistry*, 41, 1355-1379, 10.1016/j.soilbio.2009.02.031, 2009.
- Manzoni, S., Schimel, J. P., and Porporato, A.: Responses of soil microbial communities to water stress: results from a 730 meta-analysis, *Ecology*, 93, 930-938, 10.1890/11-0026.1, 2012.
- Manzoni, S., Capek, P., Mooshammer, M., Lindahl, B. D., Richter, A., and Santruckova, H.: Optimal metabolic regulation along resource stoichiometry gradients, *Ecology Letters*, 20, 1182-1191, 10.1111/ele.12815, 2017.
- Mayes, M. A., Heal, K. R., Brandt, C. C., Phillips, J. R., and Jardine, P. M.: Relation between Soil Order and Sorption of Dissolved Organic Carbon in Temperate Subsoils, *Soil Science Society of America Journal*, 76, 1027-1037, 735 10.2136/sssaj2011.0340, 2012.
- Michalzik, B., Tipping, E., Mulder, J., Lancho, J. G., Matzner, E., Bryant, C., Clarke, N., Lofts, S., and Esteban, M. V.: Modelling the production and transport of dissolved organic carbon in forest soils, *Biogeochemistry*, 66, 241-264, 2003.

- Minasny, B., Malone, B. P., McBratney, A. B., Angers, D. A., Arrouays, D., Chambers, A., Chaplot, V., Chen, Z.-S., Cheng, K., Das, B. S., Field, D. J., Gimona, A., Hedley, C. B., Hong, S. Y., Mandal, B., Marchant, B. P., Martin, M., McConkey, B. G., Mulder, V. L., O'Rourke, S., Richer-de-Forges, A. C., Odeh, I., Padarian, J., Paustian, K., Pan, G., Poggio, L., Savin, I., Stolbovoy, V., Stockmann, U., Sulaeman, Y., Tsui, C.-C., Vågen, T.-G., van Wesemael, B., and Winowiecki, L.: Soil carbon 4 per mille, *Geoderma*, 292, 59-86, 10.1016/j.geoderma.2017.01.002, 2017.
- 740 Minx, J. C., Lamb, W. F., Callaghan, M. W., Fuss, S., Hilaire, J., Creutzig, F., Amann, T., Beringer, T., de Oliveira Garcia, W., Hartmann, J., Khanna, T., Lenzi, D., Luderer, G., Nemet, G. F., Rogelj, J., Smith, P., Vicente Vicente, J. L., Wilcox, J., and del Mar Zamora Dominguez, M.: Negative emissions—Part 1: Research landscape and synthesis, *Environmental Research Letters*, 13, 10.1088/1748-9326/aabf9b, 2018.
- 745 Moyano, F. E., Manzoni, S., and Chenu, C.: Responses of soil heterotrophic respiration to moisture availability: An exploration of processes and models, *Soil Biology and Biochemistry*, 59, 72-85, 10.1016/j.soilbio.2013.01.002, 2013.
- Muttill, N. and Jayawardena, A. W.: Shuffled Complex Evolution model calibrating algorithm: enhancing its robustness and efficiency, *Hydrological Processes*, 22, 4628-4638, 10.1002/hyp.7082, 2008.
- 750 Omondi, M. O., Xia, X., Nahayo, A., Liu, X., Korai, P. K., and Pan, G.: Quantification of biochar effects on soil hydrological properties using meta-analysis of literature data, *Geoderma*, 274, 28-34, 10.1016/j.geoderma.2016.03.029, 2016.
- Osunbitan, J., Oyedele, D., and Adekalu, K.: Tillage effects on bulk density, hydraulic conductivity and strength of a loamy sand soil in southwestern Nigeria, *Soil and Tillage Research*, 82, 57-64, 2005.
- 755 Palansooriya, K. N., Wong, J. T. F., Hashimoto, Y., Huang, L., Rinklebe, J., Chang, S. X., Bolan, N., Wang, H., and Ok, Y. S.: Response of microbial communities to biochar-amended soils: a critical review, *Biochar*, 1, 3-22, 10.1007/s42773-019-00009-2, 2019.
- Parton, W. J., Morgan, J. A., Kelly, R. H., and Ojima, D.: Modeling soil C responses to environmental change in grassland systems[M] The potential of US grazing lands to sequester carbon and mitigate the greenhouse effect, 2000.
- 760 Pei, J., Li, J., Mia, S., Singh, B., Wu, J., and Dijkstra, F. A.: Biochar aging increased microbial carbon use efficiency but decreased biomass turnover time, *Geoderma*, 382, 10.1016/j.geoderma.2020.114710, 2021.
- Press WH, Teukolsky SA, Vetterling WT and Flannery BP.: *Numerical Recipes. The arts of Scientific Computing* (3rd edition). New York, Cambridge University Press, 2007.
- Ramankutty, N., Evan, A. T., Monfreda, C., and Foley, J. A.: Farming the planet: 1. Geographic distribution of global agricultural lands in the year 2000, *Global Biogeochemical Cycles*, 22, 10.1029/2007gb002952, 2008.
- 765 Razzaghi, F., Obour, P. B., and Arthur, E.: Does biochar improve soil water retention? A systematic review and meta-analysis, *Geoderma*, 361, 10.1016/j.geoderma.2019.114055, 2020.
- Roberts, K. G., Gloy, B. A., Joseph, S., Scott, N. R., and Lehmann, J.: Life Cycle Assessment of Biochar Systems: Estimating the Energetic, Economic, and Climate Change Potential, *Environmental Science & Technology*, 44, 827-833, 10.1021/es902266r, 2010.
- 770 Roychand, P. and Marschner, P.: Respiration and sorption of water-extractable organic carbon as affected by addition of Ca<sup>2+</sup>, isolated clay or clay-rich subsoil to sand, *Pedosphere*, 24, 98-106, 2014.
- Schimel, J., Balsler, T. C., and Wallenstein, M.: Microbial stress-response physiology and its implications for ecosystem function, *Ecology*, 88, 1386-1394, 10.1890/06-0219, 2007.
- 775 Schimel, J. P. and Weintraub, M. N.: The implications of exoenzyme activity on microbial carbon and nitrogen limitation in soil: a theoretical model, *Soil Biology and Biochemistry*, 35, 549-563, 2003.
- Schmidt, M. W., Skjemstad, J. O., and Jäger, C.: Carbon isotope geochemistry and nanomorphology of soil black carbon: Black chernozemic soils in central Europe originate from ancient biomass burning, *Global Biogeochemical Cycles*, 16, 70-71-70-78, 2002.
- 780 Setia, R., Rengasamy, P., and Marschner, P.: Effect of exchangeable cation concentration on sorption and desorption of dissolved organic carbon in saline soils, *Science of the Total Environment*, 465, 226-232, 2013.
- Shangguan, W., Dai, Y., Duan, Q., Liu, B., and Yuan, H.: A global soil data set for earth system modeling, *Journal of Advances in Modeling Earth Systems*, 6, 249-263, 10.1002/2013ms000293, 2014.
- Shen, Y.-H.: Sorption of natural dissolved organic matter on soil, *Chemosphere*, 38, 1505-1515, 1999.

- 785 Sheng, Y. and Zhu, L.: Biochar alters microbial community and carbon sequestration potential across different soil pH, *Sci Total Environ*, 622-623, 1391-1399, 10.1016/j.scitotenv.2017.11.337, 2018.
- Singh, B. P. and Cowie, A. L.: Long-term influence of biochar on native organic carbon mineralisation in a low-carbon clayey soil, *Scientific reports*, 4, 1-9, 2014.
- Six, J., Elliott, E., and Paustian, K.: Aggregate and soil organic matter dynamics under conventional and no - tillage systems, *Soil Science Society of America Journal*, 63, 1350-1358, 1999.
- 790 Smith, P.: Soil carbon sequestration and biochar as negative emission technologies, *Glob Chang Biol*, 22, 1315-1324, 10.1111/gcb.13178, 2016.
- Song, G., Li, L., Pan, G., and Zhang, Q.: Topsoil organic carbon storage of China and its loss by cultivation, *Biogeochemistry*, 74, 47-62, 10.1007/s10533-004-2222-3, 2005.
- 795 Sulman, B. N., Moore, J. A. M., Abramoff, R., Averill, C., Kivlin, S., Georgiou, K., Sridhar, B., Hartman, M. D., Wang, G., Wieder, W. R., Bradford, M. A., Luo, Y., Mayes, M. A., Morrison, E., Riley, W. J., Salazar, A., Schimel, J. P., Tang, J., and Classen, A. T.: Multiple models and experiments underscore large uncertainty in soil carbon dynamics, *Biogeochemistry*, 141, 109-123, 10.1007/s10533-018-0509-z, 2018.
- Sun, W., Canadell, J. G., Yu, L., Yu, L., Zhang, W., Smith, P., Fischer, T., and Huang, Y.: Climate drives global soil carbon sequestration and crop yield changes under conservation agriculture, *Glob Chang Biol*, 26, 3325-3335, 10.1111/gcb.15001, 2020.
- 800 Wang, G., Post, W. M., and Mayes, M. A.: Development of microbial-enzyme-mediated decomposition model parameters through steady-state and dynamic analyses, *Ecological Applications*, 23, 255-272, 10.1890/12-0681.1, 2013.
- Wang, G., Huang, W., Zhou, G., Mayes, M. A., and Zhou, J.: Modeling the processes of soil moisture in regulating microbial and carbon-nitrogen cycling, *Journal of Hydrology*, 585, 10.1016/j.jhydrol.2020.124777, 2020a.
- 805 Wang, J., Xiong, Z., and Kuzyakov, Y.: Biochar stability in soil: meta-analysis of decomposition and priming effects, *Global Change Biology Bioenergy*, 8, 512-523, 10.1111/gcbb.12266, 2016.
- Wang, X., He, C., Liu, B., Zhao, X., Liu, Y., Wang, Q., and Zhang, H.: Effects of Residue Returning on Soil Organic Carbon Storage and Sequestration Rate in China's Croplands: A Meta-Analysis, *Agronomy-Basel*, 10, 10.3390/agronomy10050691, 2020b.
- 810 Wieder, W. R., Bonan, G. B., and Allison, S. D.: Global soil carbon projections are improved by modelling microbial processes, *Nature climate change*, 3, 909-912, 2013.
- Wieder, W. R., Grandy, A. S., Kallenbach, C. M., and Bonan, G. B.: Integrating microbial physiology and physio-chemical principles in soils with the MIMICs model, *Biogeosciences*, 11, 3899-3917, 10.5194/bg-11-3899-2014, 2014.
- 815 Wieder, W. R., Grandy, A. S., Kallenbach, C. M., Taylor, P. G., and Bonan, G. B.: Representing life in the Earth system with soil microbial functional traits in the MIMICs model, *Geoscientific Model Development*, 8, 1789-1808, 10.5194/gmd-8-1789-2015, 2015.
- Wieder, W. R., Sulman, B. N., Hartman, M. D., Koven, C. D., and Bradford, M. A.: Arctic soil governs whether climate change drives global losses or gains in soil carbon, *Geophysical Research Letters*, 46, 14486-14495, 2019.
- 820 Woolf, D. and Lehmann, J.: Modelling the long-term response to positive and negative priming of soil organic carbon by black carbon, *Biogeochemistry*, 111, 83-95, 10.1007/s10533-012-9764-6, 2012.
- Woolf, D., Amonette, J. E., Street-Perrott, F. A., Lehmann, J., and Joseph, S.: Sustainable biochar to mitigate global climate change, *Nat Commun*, 1, 56, 10.1038/ncomms1053, 2010.
- 825 Yan, Z., Bond-Lamberty, B., Todd-Brown, K. E., Bailey, V. L., Li, S., Liu, C., and Liu, C.: A moisture function of soil heterotrophic respiration that incorporates microscale processes, *Nat Commun*, 9, 2562, 10.1038/s41467-018-04971-6, 2018.
- Yoo, G., Kim, H., and Choi, J. Y.: Soil Aggregate Dynamics Influenced by Biochar Addition using the  $^{13}\text{C}$  Natural Abundance Method, *Soil Science Society of America Journal*, 81, 612-621, 10.2136/sssaj2016.09.0313, 2017.
- 830 Zhang, H., Goll, D. S., Wang, Y. P., Ciais, P., Wieder, W. R., Abramoff, R., Huang, Y., Guenet, B., Prescher, A. K., Viscarra Rossel, R. A., Barre, P., Chenu, C., Zhou, G., and Tang, X.: Microbial dynamics and soil physicochemical properties

- explain large-scale variations in soil organic carbon, *Glob Chang Biol*, 10.1111/gcb.14994, 2020.
- Zhang, Y., Sun, C. X., Chen, L., and Duan, Z.: Catalytic potential of soil hydrolases in northeast China under different soil moisture conditions, *Revista de la ciencia del suelo y nutrición vegetal*, 9, 116-124, 2009.
- 835 Zhao, M. and Running, S. W.: Drought-induced reduction in global terrestrial net primary production from 2000 through 2009, *Science*, 329, 940-943, 10.1126/science.1192666, 2010.
- Zheng, H., Wang, X., Luo, X., Wang, Z., and Xing, B.: Biochar-induced negative carbon mineralization priming effects in a coastal wetland soil: Roles of soil aggregation and microbial modulation, *Sci Total Environ*, 610-611, 951-960, 10.1016/j.scitotenv.2017.08.166, 2018.
- 840 Zhou, H., Zhang, D., Wang, P., Liu, X., Cheng, K., Li, L., Zheng, J., Zhang, X., Zheng, J., and Crowley, D.: Changes in microbial biomass and the metabolic quotient with biochar addition to agricultural soils: A Meta-analysis, *Agriculture, Ecosystems & Environment*, 239, 80-89, 10.1016/j.agee.2017.01.006, 2017a.
- Zhou, M., Zhu, B., Wang, S., Zhu, X., Vereecken, H., and Bruggemann, N.: Stimulation of N<sub>2</sub>O emission by manure application to agricultural soils may largely offset carbon benefits: a global meta-analysis, *Glob Chang Biol*, 23, 845 4068-4083, 10.1111/gcb.13648, 2017b.
- Zimmerman, A. R., Gao, B., and Ahn, M.-Y.: Positive and negative carbon mineralization priming effects among a variety of biochar-amended soils, *Soil Biology and Biochemistry*, 43, 1169-1179, 10.1016/j.soilbio.2011.02.005, 2011.
- Zomer, R. J., Xu, J., and Trabucco, A.: Version 3 of the Global Aridity Index and Potential Evapotranspiration Database, *Sci Data*, 9, 409, 10.1038/s41597-022-01493-1, 2022.

850